Hydrodynamic Performances of KRISO Container Ship (KCS) Using CAD-CAE and CFD Techniques

Hassiba OUARGLI

Master Thesis

presented in partial fulfilment
of the requirements for the double degree:
“Advanced Master in Naval Architecture” conferred by University of Liege
"Master of Sciences in Applied Mechanics, specialization in Hydrodynamics, Energetic and Propulsion” conferred by Ecole Centrale de Nantes

developed at "Dunarea de Jos" University of Galati
in the framework of the

“EMSHIP”
Erasmus Mundus Master Course
in “Integrated Advanced Ship Design”

Ref. 159652-1-2009-1-BE-ERA MUNDUS-EMMC

Supervisor:	Prof. Dan Obreja, "Dunarea de Jos" University of Galati Prof. Florin Pacurau, "Dunarea de Jos" University of Galati
Reviewer:	Prof. Robert Bronsart, University of Rostock

Galati, February 2015

ABSTRACT

Hydrodynamic Performances of KRISO Container Ship (KCS) Using CAD-CAE and CFD Techniques

By **Hassiba OUARGLI**

Key Words: KCS, Resistance, Powering, Manoeuvring, Potential flow, Viscous flow.

While at the initial design stage one has to rely on systematic experience, empirical methods and experimental model tests to predict ship hydrodynamics performance, it is now becoming more and more common to involve CFD methods in order to optimise the body lines plan.

The KCS container ship was designed at the KRISO (Korea Research Institute for Ships and Ocean Engineering), now MOERI (Maritime and Ocean Engineering Research Institute), that can be used as a benchmark model for CFD predictions.

The aim of this thesis is to compute with preliminary design tools and CFD instruments the hydrodynamic performances (resistance, powering and manoeuvrability) of the KCS container ship and to validate some numerical results on the basis of the model resistance tests performed both at the small Towing Tank from *Dunarea de J*os University of Galati (45 m in length) and at the large Towing Tank from MOERI. The goal of the comparison is to evaluate the chances that a small basin like the one in Galati has to accurately predict the hydrodynamic resistance for this type of ship.

The preliminary hydrodynamic performances are computed using the hydrodynamic modules of AVEVA Initial Design system, on the basis of the main dimensions, hydrostatics characteristics and the body lines plan of the KCS container ship.

Also, the CFD instruments may be used as a predictive tool and the naval architects must have confidence that the simulation results are an accurate representation of reality. SHIPFLOW code has been applied directly to full scale, in order to study the free surface potential flow and viscous flow around the KCS hull, delivering the ship resistance. The numerical results have been validated using experimental data bases, including experimental tests results obtained at the Towing Tank from Galati University, with a model having 3.502 m length and at the MOERI Towing Tank, for a KCS model with 7.279 m length.

The comparison between numerical and experimental results suggests the necessity to improve the preliminary design tools and the CFD methods in order to obtain realistic prediction of the hydrodynamics performances of the large ships. Also, the small towing tank from Galati University can be used in order to predict with satisfactory accuracy the resistance for this type of ships'.

ACKNOWLEDGEMENTS

The author would like to acknowledge the following honourable dignitaries and professors for their benevolent help towards the success of the thesis:

1. Professor Philippe Rigo (ULG, Belgium.)

2. Professor Dan Constantin Obreja (UGAL, Romania.)

3. Professor Florin Pacuraru (UGAL, Romania.)

4. Professor Mihaela Amoraritei (UGAL, Romania.)

5. Professor Leonard Domnisoru (UGAL, Romania.)

6. Mr.Vasilea Giuglea (Managing Director at S.D.G, Romania.)

7. Mr.Stefan Giuglea (Deputy Managing Director at S.D.G, Romania.)

8. Dr. Ionas Ovidiu (Technical director at S.D.G, Romania.)

TABLE OF CONTENTS

Declaration of Authorship

I Hassiba OUARGLI declare that this thesis and the work presented in it are my own and have been generated by me as the result of my own original research.

"Hydrodynamic Performances Of KRISO Container Ship (KCS) Using CAD-CAE And CFD Techniques"

Where I have consulted the published work of others, this is always clearly attributed.

Where I have quoted from the work of others, the source is always given. With the exception of such quotations, this thesis is entirely my own work.

I have acknowledged all main sources of help.

Where the thesis is based on work done by myself jointly with others, I have made clear exactly what was done by others and what I have contributed myself.

This thesis contains no material that has been submitted previously, in whole or in part, for the award of any other academic degree or diploma.

I cede copyright of the thesis in favour of the University of "Dunarea de Jos" University of Galati

Date: 29.01.2015 *Signature*

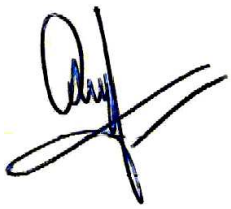

LIST OF FIGURES

LIST OF TABLES

1 INTRODUCTION

Hydrodynamic aspects play a significant role in the quality of a ship. Dominant criteria in the hull form design are resistance and powering performances, as well as the occurrence of noise and vibrations, which are important for the comfort level of crew and passengers [1].

The development of the CFD techniques have given progress in modelling free-surface flow around ship hull and numerical prediction of ship resistance. Even the experimental modelling it has its relevance, being required to validate the numerical prediction and estimation of ship resistance.

The KCS container ship was designed at the KRISO (Korea Research Institute for Ships and Ocean Engineering), now MOERI (Maritime and Ocean Engineering Research Institute), in order to be used as a benchmark model for CFD predictions.

The hydrodynamic performances (resistance, powering, and manoeuvrability) of the KCS hull are computed using a preliminary prediction method in AVEVA Initial Design system Tribon M3, on the basis of the body lines plan, The numerical results are validated using experimental data bases, including model experimental tests results obtained at the Towing Tank from Galati University.

The free surface study (potential flow and viscous flow) is carried out using CFD method by SHIPFLOW code. This study is important in the initial design stage for new hull forms obtained by modifying the basic hull forms which are already based on experiences and on databases. With the additional modifications of the hull form, we have to confirm that the new designs meet the demands of performances (flow field, pressure field, speed, resistance … etc.) [2].

1.1 Justification

While at the early design stages one has to rely on systematic experience, empirical methods or conduct model tests for ship performance prediction, it is now becoming more and more common to involve CFD methods for the check of the design and for solving optimization problems where changes of hull and propeller designs are required. CFD methods allow the simulation of the whole system ship-propulsion including all significant mechanisms that influence its performance, such as turbulence, free surface, interaction effects and cavitations.

These methods can be applied directly to full scale, and they can be used in scale effect studies [4].

The preliminary hydrodynamic performances are computed using the hydrodynamic modules of AVEVA Initial Design system, on the basis of the main dimensions, hydrostatic characteristics and the body lines plan of the KCS container ship.

Also, the CFD instruments may be used as a predictive tool and the naval architects must have confidence that the simulation results are an accurate representation of reality. SHIPFLOW code has been applied directly to full scale, in order to study the free surface potential flow and viscous flow around the KCS hull, including the ship resistance.

1.2 Objectives

The Korean Research Institute for Ships and Ocean Engineering (KRISO) container ship KCS is considered as a modern container ship. The studies of this hull in the thesis will be focus on hydrodynamic performances: (powering, resistances, manoeuvrability) and free surface around the hull (potential flow and viscous flow).

The ‘igs’ file of the hull is obtained from the database of KRISO website, and used for CFD simulations by extracting lines plan from this file that are used for hydrodynamic performances analysis using AVEVA-TribonM3.

This master thesis is divided on six chapters presented as follows:

Chapter one: introduction and general presentation of the KCS hull benchmark, objectives of thesis.

Chapter two: preliminary hydrodynamic performances: there is the preliminary estimation for the KCS hull, carried out using mathematical models of CAD_CAE techniques for initial design AVEVA-Tribon M3; using these tools, we performed the following studies: ship resistance and powering, calculation of the resistance and the power, manoeuvring performances, turning circle manoeuvre, zig-zag and spiral manoeuvre.

Chapter three: CFD potential flow simulation using SHIPFLOW code on the container ship KCS without propeller with free surface at full scale, there were used three sets of grids, the results were provided according to the ITTC recommended procedures and guidelines.

Chapter four: CFD viscous flow simulation: for the same three sets of grid there are carried out viscous flow simulation.

Chapter five: resistance test for the KCS model was performed at towing tank from University of Galati, a comparative study of the numerical and experimental results from both towing tanks of University of Galati and MOERI towing tank in Korea is carried out.

Chapter six: general conclusions and future recommendations.

1.3 KCS Benchmark

The KCS was conceived to provide data both for explication of flow physics and CFD validation for a modern container ship ca. 1997 with bulb bow and stern. The Korea Research Institute for Ships and Ocean Engineering (now MOERI) performed towing tank experiments to obtain resistance, mean flow data and free surface waves (Van et al 1998, Kim et al 2001). Self-propulsion tests were carried out at the Ship Research Institute (now NMRI) in Tokyo and have been reported in the proceeding of the CFD Workshop Tokyo in 2005 (Hino 2005). Data for pitch, heave, and added resistance are also already available from Force/DMI measurements reported in Simonsen et al (2008). All these studies have been attended also on a full scale ship [1], a conventional container ship, KRISO (KCS, LBP=230m and 7.287m for full and model scales), The KCS hull form was for the first time selected at the Gothenburg 2000 workshop for a modern slender ship case as a replacement for the Series 60 (Cb = 0.6) model, as in the earlier workshop [2].

The KCS hull is characterized by its long bulbous bow, and it's extended stern overhang which makes new design but produces complex flow behind the hull and wake fields [2].

The main characteristics of the hull shapes are presented below in the Table 1. [1].

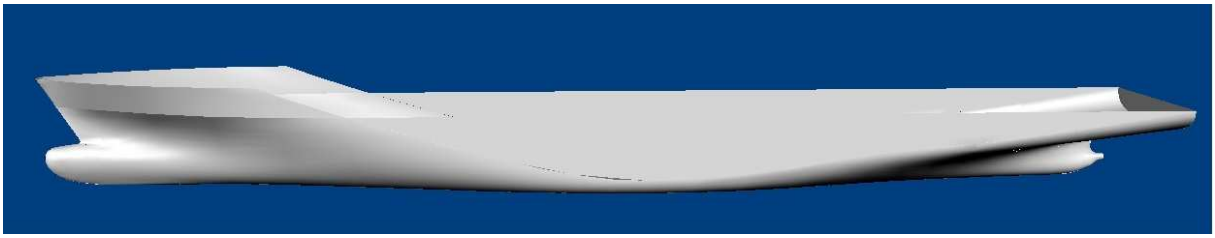

Figure 1.KRISO Container Ship KCS Hull.

Table 1. Main dimensions of the KCS [3].

Main characteristics	**Full scale**	**Model scale**	**1/65.67**
Length over all, *LOA* [m]	243.84	3.713	
Length of waterline, *LW* [m]	232.5	3.54	
Length between perpendiculars, *LBP* [m]	230.0	3.502	
Beam, *B* [m]	32.2	0.49	
Depth, *D* [m]	19.0	0.289	
Draft, *T* [m]	10.8	0.164	
Longitudinal centre of buoyancy from the aft perpendicular, *LCB* [m]	111.596	1.699	
Volumetric displacement, Ñ[m3]	52030	0.1837	
Hull wetted surface, *S* [m2]	9424.0	2.185	
Speed, *v*	24 Kn	1.523 m/s	
Froude number, *Fn*	0.26	0.26	
Block coefficient, *CB*	0.6505	0.6505	
Midship section coefficient, *CM*	0.985	0.985	

2 PRELIMINARY HYDRODYNAMICS PERFORMANCES

The hydrodynamic performances can be divided on several areas: ship resistance and powering, manoeuvrability performances, ship propulsion and seakeeping performances.

2.1 AVEVA (Tribon ID) System

The origin of the TRIBON-M3 initial design system, which is a naval architecture tools, refers to Kochum Computer System (KCS), aiming to provide a good and a structured way for developing the information between different tasks an conditions during the shipbuilding stage. KCS was separated from the shipyard Kochum, then named Tribon, and finally acquired by AVEVA in 2004.

The Tribon system uses a Product Information Model (PIM) database, which was designed to handle all the structural and outfit objects of marine and shipbuilding industry. It overcome all phases of the production and design process, and the information obtained from one stage can be used for the next stage, all in one design project.

The Tribon-M3 initial design works on three basic stages:

- Modelling of the geometry of the hull;
- Hydrostatic calculations in Tribon is (calc & hydro module);
- Hydrodynamics programs which are included in Tribon-M3 (calc & hydro).

For the **first stage** of geometry modelling there are performed:

- Form module;
- Lines module;
- Surface and compartments module.

1. The *Tribon form* module is a program based on initial general parameters, which can provide the ability of generating a complete hull form sufficient for initial calculations.
2. The *Tribon lines* module is used specifically for fairing the hull form.
3. The *Tribon surface & compartments* is used in the design stage to define quickly the decks, longitudinal and transversal bulkheads and all appendages, which are used in Tribon calc & hydro.

For the **second stage**: Tribon calc & hydro is the module of analysis and it comprises:

- Hydrostatic calculations and stability of the ship;

- Resistance performances and powering;
- Manoeuvring performances;
- Seakeeping performances.

2.2 Geometry Preparation

On Tribon-M3 we start by project creation

- Tribon Project Tool

Using this tool we create a project named KCS, by inserting initial parameters (geometrical parameters: length, beam, draught… etc.) as illustrated in Figure 2. This module creates the projects and manages them:

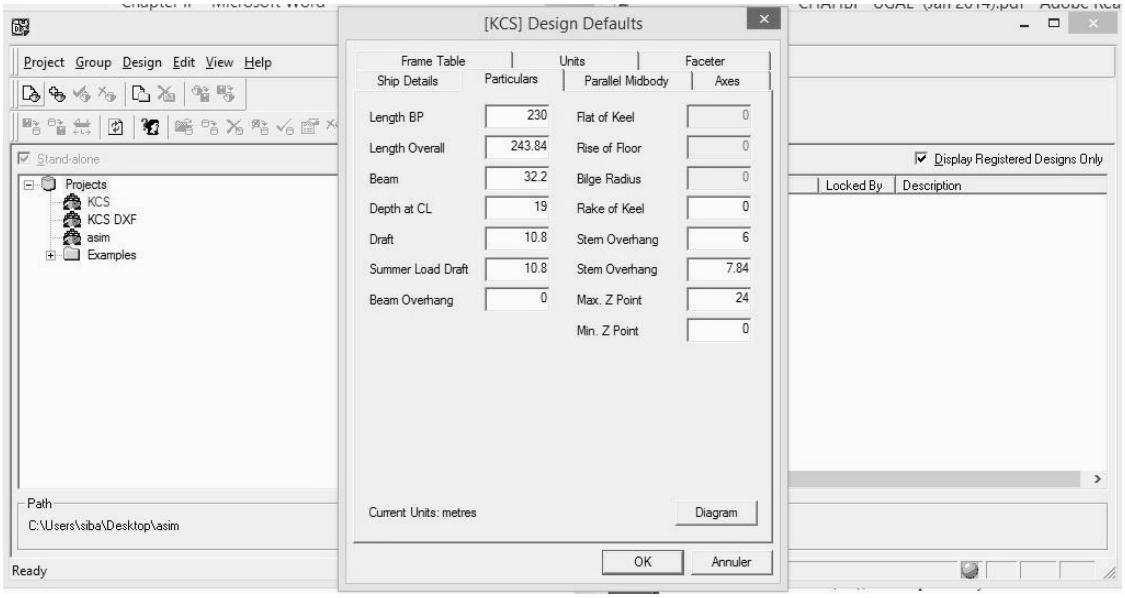

Figure 2.Initial parameters.

- Tribon lines module

Creating lines of the ship hull is the purpose of this module. This lines will be presented in a 3D geometry, by using a Britfair module file (.bri):
The Britfair file is generated by inserting points coordinates (y,z) of the lines plan:
The lines plan is generated from the offset file (.igs) existing in the KRISO website, the hull is divided on twenty section between the two aft and fore perpendiculars, see Figure 3.

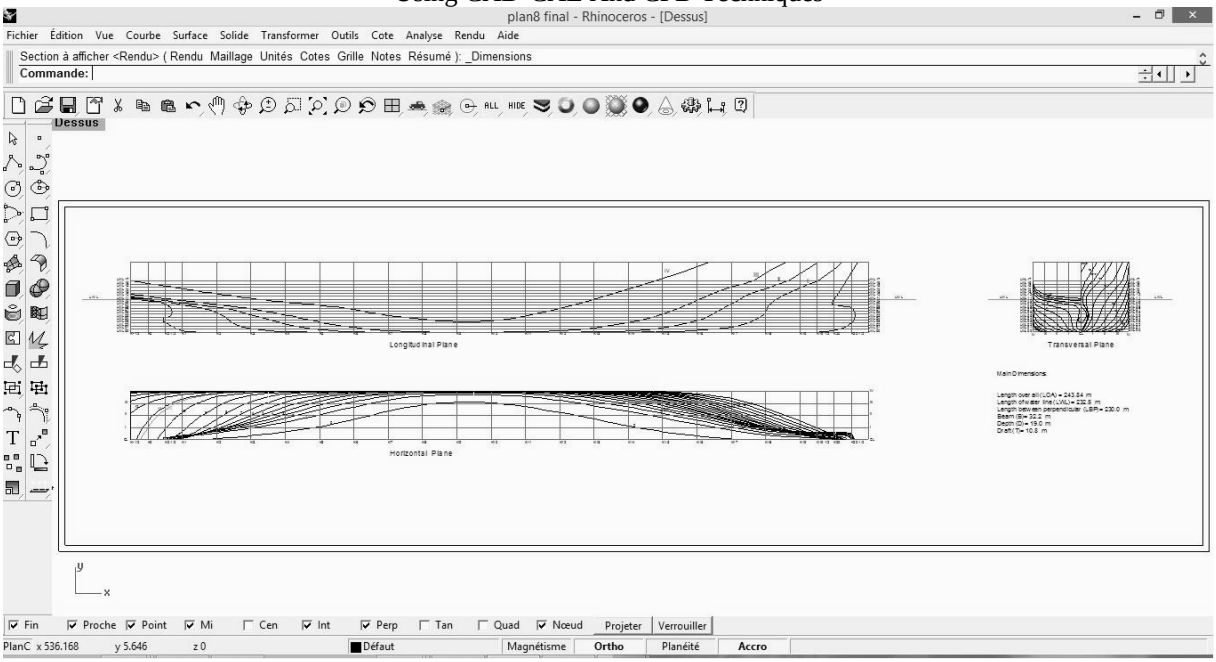

Figure 3. KCS lines plan.

From the body lines plan Rhino we insert to the britfair file point by point section by section as in Figure 4.

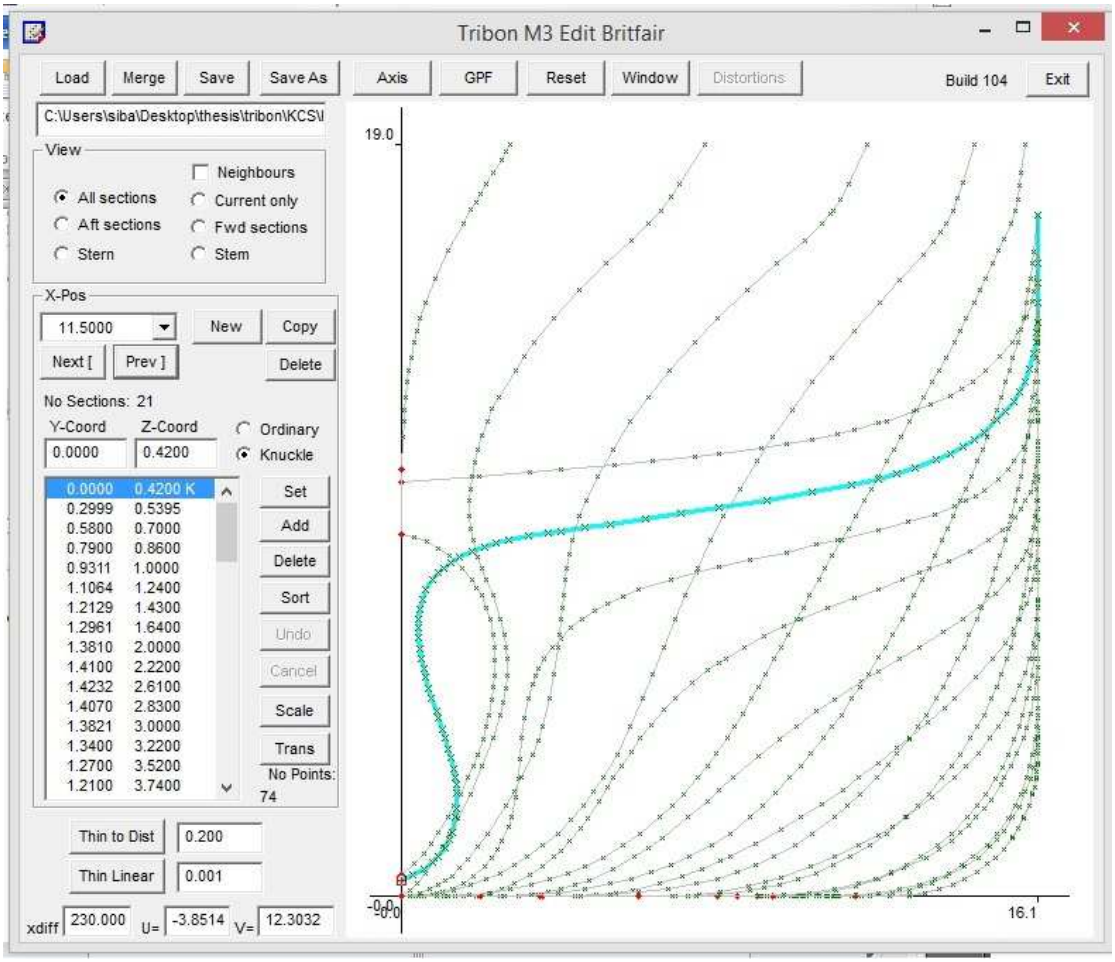

Figure 4. Britfair file generation.

On the lines module we can show the Britfair lines plan in a 3D form as seen in the Figure 5.

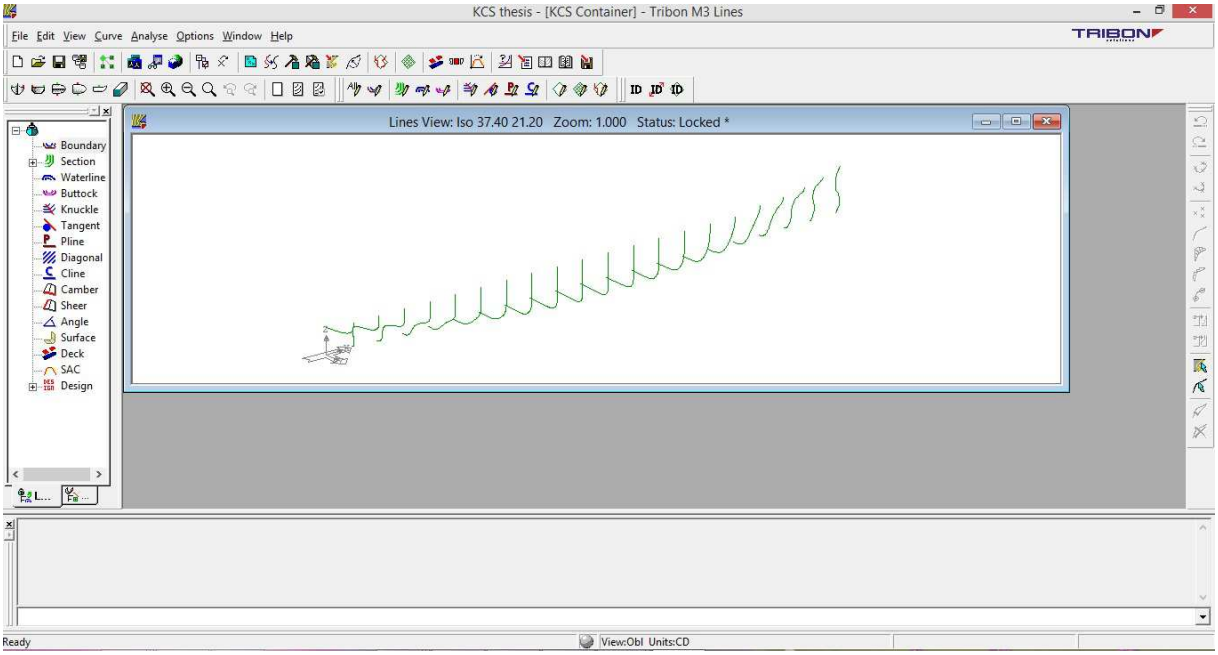

Figure 5. Lines fairing.

- Surface & compartment Tribon module

The last phase of Tribon geometry selection, it is an offset file generation of the designed ship hull made in previous modules, for directly use in calculations (calc & hydro). From a 3D lines to surface, deck points, bulkheads, compartments and appendages all can be defined in this module. See Figure 6.

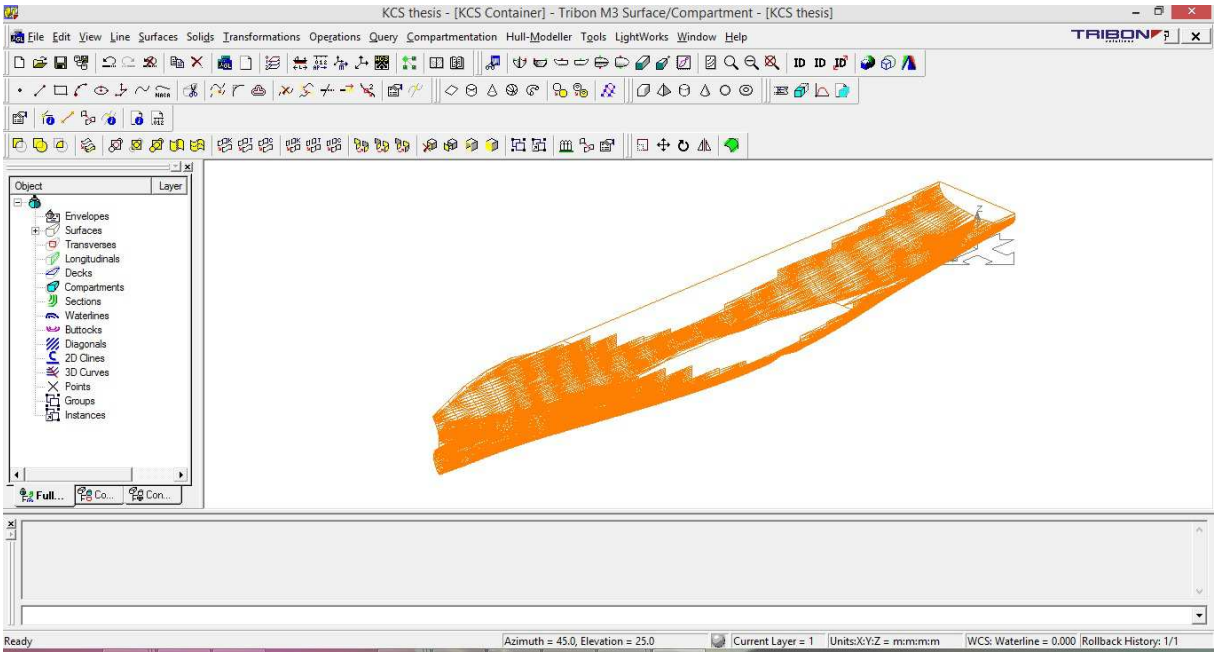

Figure 6. Surface modelling.

- Tribon-M3 calc & hydro module

This module is a very good tool for naval architects for their assessment routines which include: hydrostatic calculation, tank calibration, form calculations, stability calculations, probabilistic stability, loading conditions. See Figure 7.

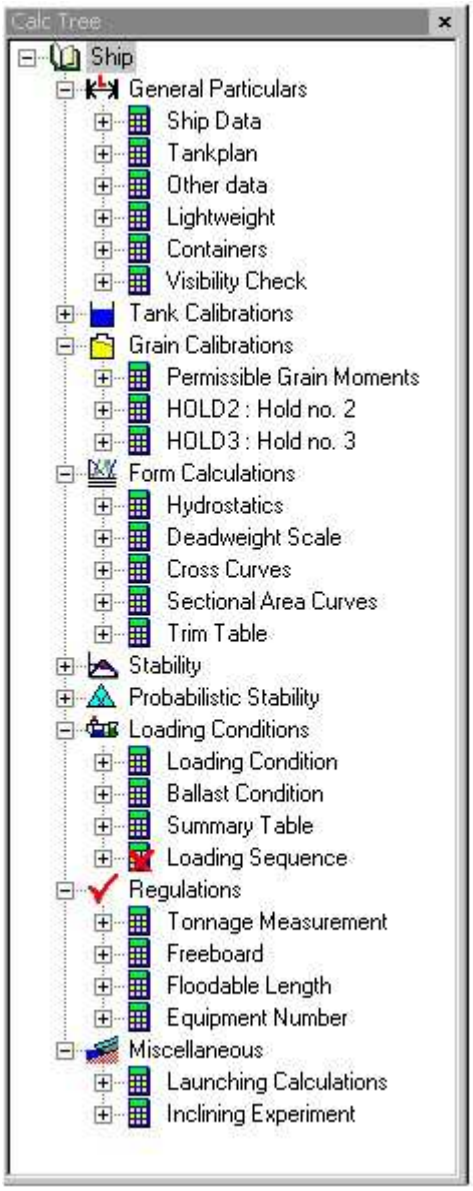

Figure 7. Different assessments modules of Tribon-M3.

The calc & hydro module is used beside the geometry data of the KCS hull, from the surface & compartments module with the following particulars in the Tables: 2, 3, 4, 5, 6, 7.

Table 2. Main dimensions of KCS in the Tribon modules.

Length Overall	243.840	metres
Length B.P	230.000	metres
Breadth mld.	32.200	metres
Depth mld.	19.000	metres
Design Draft (moulded)	10.800	metres
Summer Load Draft (extreme)	10.800	metres
Displacement at Load Draft	53045	tonnes
Lightship Weight	0	tonnes
Deadweight at Load Draft	53045	tonnes
Subdivision Length (Ls)	230.000	metres
Aft end of Ls aft of AP	0.000	metres
Subdivision Load Line (ds)	10.800	metres
Lightest Service Draft (d0)	7.560	metres

Table 3. Axis convention.

Origin from AP	0.000	metres
Positive x-direction	Aft to Forward	
Positive y-direction	Port to Stbd.	

Table 4. See water properties.

Sea water density	1.02500	tonnes/cu.m
Temperature	15.00	degs. C

Table 5. Balancing tolerances.

Draft tolerance	0.001	metres
Trim tolerance	0.010	metres
Heel increment	5.000	degs
Max. no. iterations	20	

Table 6. Draft marks aft.

x-value (m)	z-value (m)
0.000	0.000

Table 7. Draft marks Fwd.

x-value (m)	z-value (m)
230.000	0.000

2.3 Hydrostatic Calculations

The hydrostatic particulars are calculated for the hull at separated intervals, in function of drafts, and for a single no trim and no heel condition. These particulars will be plotted in the hydrostatic curves Figure 8 and tables (see APPENDIX AN1).

2.3.1 Hydrostatic Curves

In this thesis we use the hydrostatic section from calc & hydro module:
The input file from the first stage of hull geometry model will be integrated to the Calc & hydro – hydrostatic calculations.
The dialog displays a list of drafts, in unit increments and in ascending order of depth. This list is automatically created by Calc based on the principal dimensions of the hull form as contained in the input hull geometry model. The User can either accept the full list of drafts or he can select only those that he wishes to use in the subsequent hydrostatic calculations. Up to a maximum of 1000 output drafts can be specified. Also, he can elect to base the hydrostatic calculations on the moulded hull form, or can allow for the average shell plate thickness by inputting an estimated value on the Ship Data node
Different particulars in hydrostatic curves are plotted vs drafts, and are listed as below:
Δ: The displacement.
LCB: The longitudinal centre of buoyancy.
VCB: The vertical centre of buoyancy.
LCF: The longitudinal centre of flotation.
KML: The longitudinal height of metacentre.
KMT: The transversal height of metacentre.
WPA: The water plane area.
WSA: The wetted surface area.
TPC: The tonnes per centimetre immersion.
MTC: The moment to change trim one centimetre.
The following Table 8 gives a list if units and terminology used in calc & hydro for hydrostatic calculations, where LBP is the length between the two perpendiculars AP and FP.

Table 8. Terminology of calc & hydro module.

SYMBOL	*DESCRIPTION*	*UNIT*
DRAFT	the moulded draft at midships (LBP/2). Measured normal to the baseline	[m]
DISPLT	the displacement of the ship in water of the specified density. The default density is - 1.025 tone/m3	[t]
TPI/TPC	the tones per centimetre immersion or the tons per inch immersion	[t]
MCT	the moment to change trim one centimetre or one inch between the perpendiculars	[tm]
LCB	the longitudinal centre of buoyancy of the moulded hull volume, i.e. including appendages and excluding shell plating. Measured from the AP, positive forwards and parallel to the baseline.	[m]
LCF	the longitudinal centre of flotation of the moulded water plane area, i.e. including appendages and excluding shell plating. Measured from the AP, positive forwards and parallel to the baseline.	[m]
TCF	the transverse centre of flotation of the moulded water plane area, i.e. including appendages and excluding shell plating. Measured normal to the centre line, positive to starboard.	[m]
KM_L	the height of the longitudinal meta centre above the moulded baseline at midships. The moulded hull water plane area and volume are used, i.e. including appendages but not the shell plating. **$KM_L = VCB + BM_L$**	[m]
WPA	the moulded water plane area including appendages and excluding shell plating	[m^2]
VCB	the vertical centre of buoyancy of the moulded hull volume, including appendages and excluding shell plating. Measured normal to the moulded baseline at midships.	[m]
TCB	the transverse centre of buoyancy of the moulded hull volume, including appendages and excluding shell plating. Measured normal to the centre line, positive to starboard.	[m]
BM_L	the longitudinal metacentre radius, i.e. the height of the longitudinal metacentre above the centre of buoyancy for the moulded hull	[m]
BM_T	the transverse metacentre radius, i.e. the height of the transverse metacentre above the centre of buoyancy for the moulded hull.	[m]
KMT	the height of the transverse metacentre above the moulded baseline. The moulded hull water plane area and volume are used i.e. including appendages and excluding the shell plating. **$KM_T = VCB + BM_T$**	[m]
WSA	The wetted surface area can be calculated in one of two ways : - Directly from the geometry model. - Estimated using the Denny-Mumford formula	[m^2]

In Figure 8 of hydrostatic curves, the range of draft is [0 m - 12 m] with an increment of 0.5 m, also introducing the design draft 10.8 m, as additional draft. We observe that the displacement increases proportionally with the increasing of draft, so we conclude that the

Hydrostatic curves in the figure 8 are correct. The coefficients of the hull form can be calculated from the table given in APPENDICE AN1 at the design draft 10.8 m.

The block coefficient C_B is determined by:

$$C_B = \frac{\Delta}{\rho * L * B * T} \qquad \text{Eq. 1}$$

$$C_B = 0.656$$

The water plane area coefficient is determined by:

$$C_W = \frac{WPA}{L * B} \qquad \text{Eq. 2}$$

$$C_W = 0.8196$$

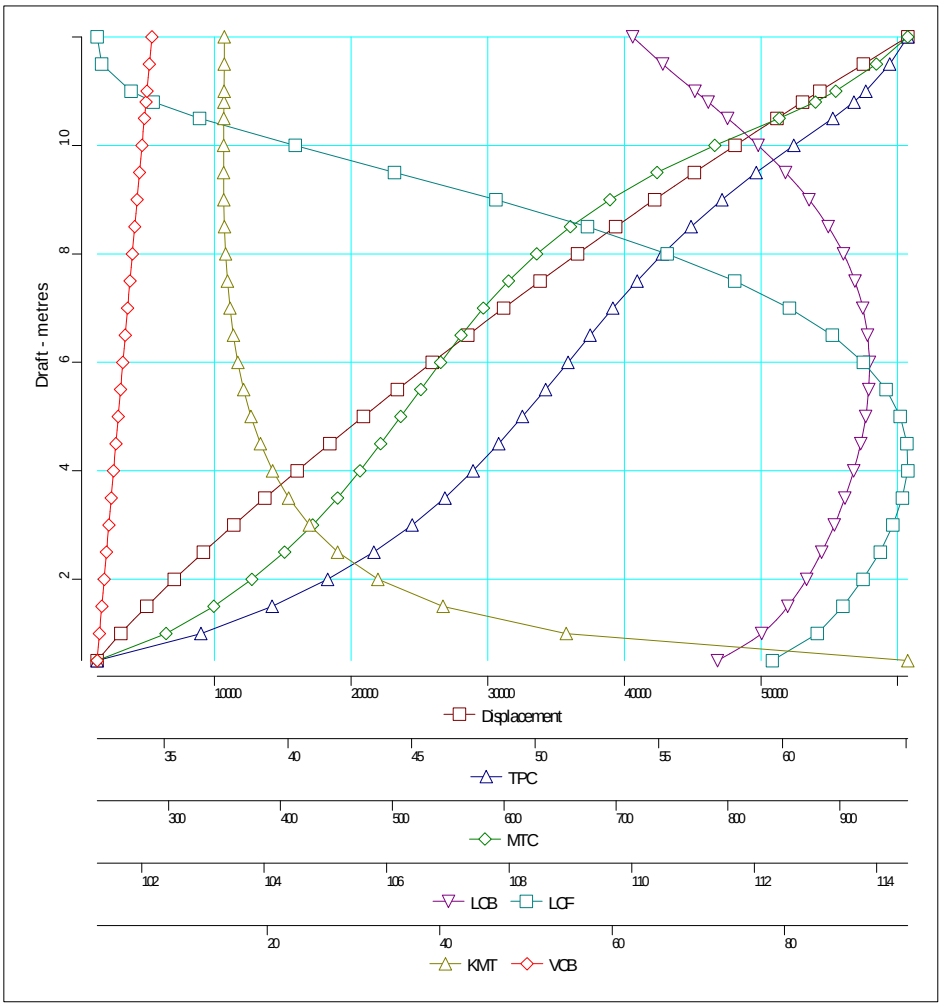

Figure 8. Hydrostatic curves.

The metacentre height GMT is determined by:

$$GM_T = KM_T - KG \qquad \text{Eq. 3}$$

$$KM_T = 14.974m$$

$$KG = coeff * D$$ Eq. 4

$$coeff = 0.74$$

$$GM_T = 0.914m \approx 1m$$

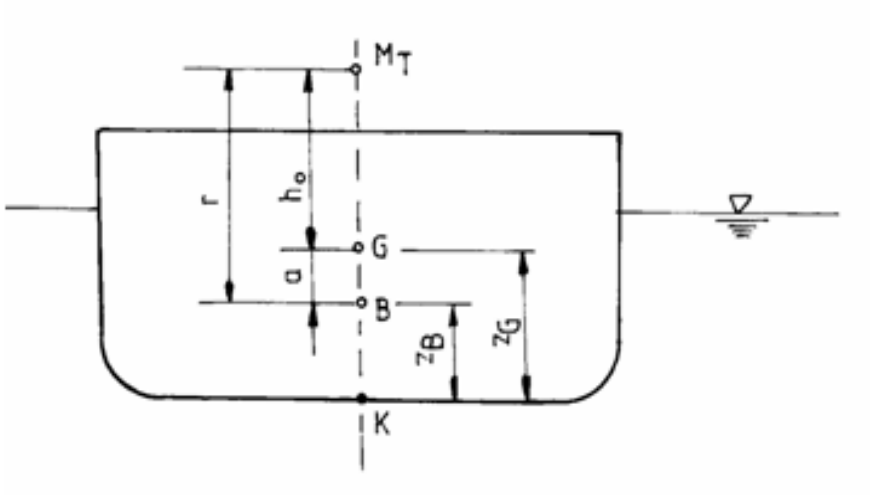

Figure 9. Metacentric height (Obreja 2003).

2.3.2 Bonjean Curves (Sectional Area Curves)

Sectional area and Bonjean curves calculation are maintained to the main hull designed for a range of draft: [0m – 19m] with 1m increment, where the designed draft 10.8 is included (for a zero trim and zero heel condition). The software defines 10 sections with increment of 0.5, means the aft and fore perpendiculars are on 0 and 10 sections respectively, and the midship section is at 5 section.

The results are presented in graphical form, with separated graphs produced for each draft in figure 10 and in the table from APPENDICE AN2, where are represented all the Bonjean's output stations.

The *midship section coefficient* is determined by:

$$C_M = \frac{AM}{B * T}$$ Eq. 5

$$AM = 342.241m^2$$

$$C_M = 0.9841$$

The *longitudinal prismatic coefficient* is determined by:

$$C_P = \frac{C_B}{C_M}$$ Eq. 6

$$C_P = 0.6665$$

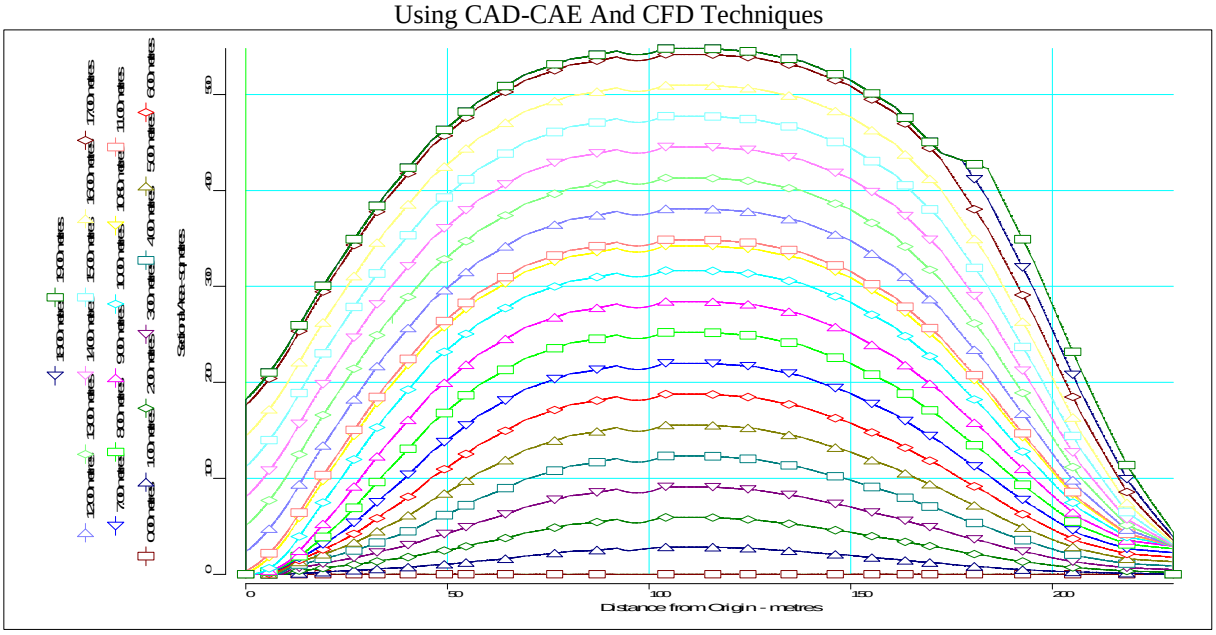

Figure 10. Bonjean curves (Sectional area) of KCS.

A comparison between the main characteristic data of the KCS and the characteristics obtained by Tribon-M3, has been done and presented in the Table 9.

Table 9. Comparison of Tribon-M3 KCS hull characteristics with the main characteristics of MOERI.

main characteristics	Full scale KCS	KCS hull modelled in Tribon-M3	difference	
Volumetric displacement ∇ (m^3)	52030	51751,73659	0,5348134	%
hull wetted surface (m^2)	9424	9506,86	-0,879244	%
block coefficient C_B	0,6505	0,656	-0,845503	%
midship section coefficient C_M	0,985	0,9841	0,0913706	%
longitudinal prismatic coefficient C_P	0,66040	0,6665	-0,922752	%

We observe that the difference between the two form characteristics is very small, which is for all coefficients less than 1%.

2.4 Ship resistance and powering

The Powering module incorporates a number of well proven empirically derived methods to predict the resistance and powering characteristics of a hull form and its associated appendages.

2.4.1 Ship resistance

The prediction of ship resistance in Tribon-M3 calc & hydro module is executed by different empirical methods.

The empirical method Holtrop and Mennen, based on statistical analysis of experiments with 191 models which are available at the Netherlands Model Basin (MARIN), was used in order to compute the KCS ship resistance. Accuracy of this method results are satisfactory at preliminary design for about 95% of the cases studied in a range of hull parameters as shown in the Table 10.

Table 10. KCS according to the Holtrop and Mennen limitations.

Holtrop and Mennen method	KCS
Fn≤0.45	0.26
0.55≤CP≤0.67	0.6665
6.0≤L/B≤9.5	7.1
3.0≤B/T≤4.0	2.98

The KCS hull parameters are compatible with the range of the Holtrop and Mennen.

The total resistance of the ship is calculated as follow:

$$R_{TOTAL} = R_F(1+k_1) + R_W + R_B + R_{TR} + R_A \qquad \text{Eq. 7}$$

Where :

R_F : Frictional resistance;

$(1+k_1)$: Form factor, for the viscous resistance computation;

R_W : Wave resistance;

R_B : Additional pressure resistance of the bulbous bow;

R_{TR} : Additional pressure resistance of the immersed transom;

R_A : Ship-model correlation resistance.

In the Tribon-M3 calc & hydro the inputs are: ship form coefficients, ship speed range [14 Knts – 26 Knts] with step of 1 Knts and bulbous bow information, see Tables: 11-12-13.

Table 11. Physical constants.

Grav. accel (g)	9.81000	metres/sec^2
Water temperature	15.0	deg.C
Water density	1.02500	tonnes/cu.m
Water viscosity	1.1883e-006	metres^2/sec

Table 12. The input data condition- resistance module.

Draught aft	10.800	metres	
Draught fwd	10.800	metres	
Mean draught	10.800	metres	
Length aft of AP	2.490	metres	
Length fwd of FP	0.000	metres	
Transom area	0.000	sq.metres	(0.000 % midship area)
Bulb area	22.500	sq.metres	(6.470 % midship area)
Height of Centroid	5.600	metres	
Displacement	53046	tonnes	
Long. centre buoy.	-3.753	metres	(-1.632 % LPP fwd midships)
Wetted surface	9507	sq.metres	
Half entrance angle	17.600	degrees	

Table 13. Appendages.

Appendage name	Surface Area (m^2)	1+k2
Rudder	54.450	1.750
Total	**54.450**	**1.750**

The Holtrop-Mennen formula estimate the form factor K:

Form factor, k	0.185

The resistance coefficients are obtained from the Holtrop-Mennen, see Table 14 below:

Table 14.KCS Resistance coefficients

Speed kts	Fn	Rn /10^9	Cf *10^3	Cf x k *10^3	Cr *10^3	Ca *10^3	Ct *10^3
14.000	0.151	1.409	1.468	0.272	0.068	0.320	2.142
15.000	0.162	1.510	1.455	0.270	0.091	0.320	2.150
16.000	0.172	1.610	1.444	0.268	0.123	0.320	2.169
17.000	0.183	1.711	1.433	0.266	0.165	0.320	2.198
18.000	0.194	1.812	1.424	0.264	0.218	0.320	2.240
19.000	0.205	1.912	1.415	0.262	0.283	0.320	2.294
20.000	0.215	2.013	1.406	0.261	0.361	0.320	2.361
21.000	0.226	2.114	1.398	0.259	0.447	0.320	2.438
22.000	0.237	2.214	1.390	0.258	0.539	0.320	2.520
23.000	0.248	2.315	1.383	0.256	0.644	0.320	2.616
24.000	0.259	2.416	1.376	0.255	0.777	0.320	2.741
25.000	0.269	2.516	1.369	0.254	0.938	0.320	2.895
26.000	0.280	2.617	1.363	0.253	1.105	0.320	3.054

From these results the resistances are calculated by using these formulas:

$$R_F = \frac{1}{2} * \rho * V^2 * WSA * C_F \quad \text{Eq. 8}$$

$$R_W = \frac{1}{2} * \rho * V^2 * WSA * C_W \quad \text{Eq. 9}$$

$$R_A = \frac{1}{2} * \rho * V^2 * WSA * C_A \quad \text{Eq. 10}$$

$$R_T = \frac{1}{2} * \rho * V^2 * WSA * C_T \quad \text{Eq. 11}$$

Where :

V: the ship speed;

WSA: Wetted surface area;

C: specific resistance coefficients.

The computed results are presented in Table 15.

Table 15. KCS Ship resistance components.

V Knts	Rf*(1+k)	Rw	Ra	Rb	Rt
14	439,5754	17,18296	80,86097	3,643797	541,2631
15	500,1459	26,39714	92,82509	4,300412	623,6686
16	564,7528	40,59551	105,6143	4,904465	715,8671
17	632,6963	61,47728	119,2287	5,549722	818,9519
18	704,8655	91,06141	133,6681	6,0819	935,6769
19	780,3957	131,7124	148,9327	6,620524	1067,661
20	859,2045	186,1659	165,0224	7,163003	1217,556
21	941,8831	254,1435	181,9372	8,170116	1386,134
22	1027,807	336,3311	199,6771	8,642274	1572,457
23	1117,71	439,2122	218,2421	8,964976	1784,129
24	1210,855	577,0008	237,6322	9,980554	2035,469
25	1307,178	755,8154	257,8475	11,87307	2332,714
26	1407,647	963,0345	278,8878	12,06626	2661,636

The total resistance is shown in the following Figure 11.

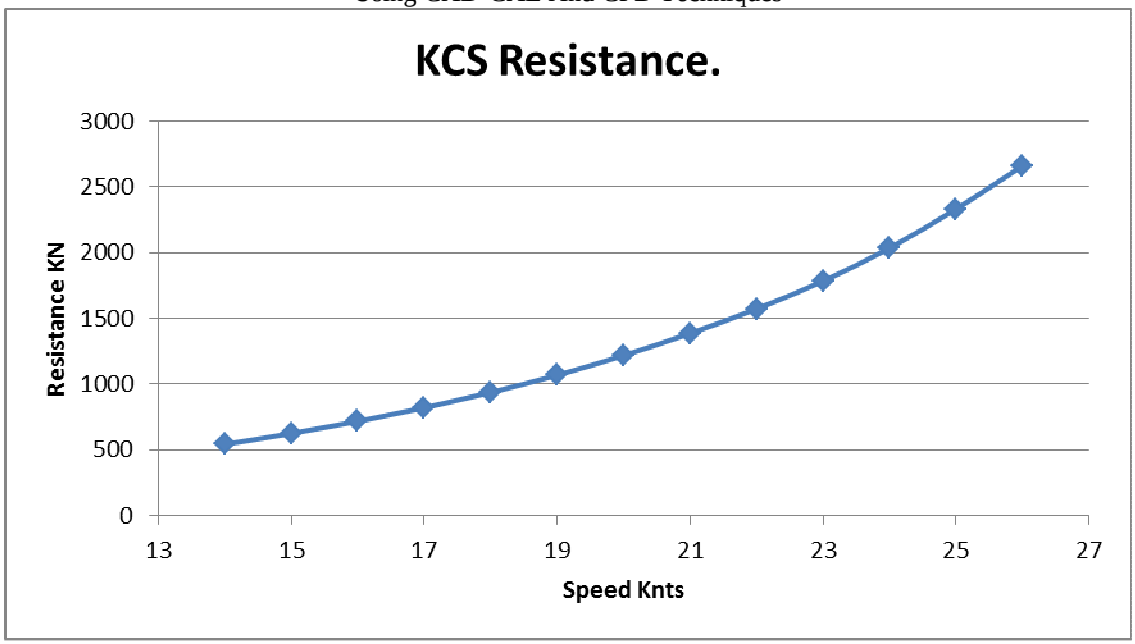

Figure 11. KCS Resistance.

2.4.2 Hydrodynamic characteristics of the propeller

The KCS optimum propeller has been design by MOERI at the draft given by the design condition. Many optimisation modes can be utilised, and there are two series available in the module Tribon-M3 calc & hydro, powering tool:

- ***Wageningen B-series***
- ***Gawn-Burrill segmental propeller series.***

The Wageningen B-series are suitable for merchant ships, whereas the Gawn-Burrill propeller series are more convenient for the warships with higher loading conditions.
Three different ways are provided to optimise the propeller:

– Given ship speed and rpm of the propeller, to determine the optimum diameter, pitch and the blade area ratio;

– Given ship speed and diameter of the propeller, to determine the optimum RPM of propeller, pitch and blade area ratio;

– Given the delivered power and RPM, to determine the optimum diameter, pitch and blade area ratio. (An estimated design speed must also be supplied as a starting point for the iteration process).

This module provides also three methods of correction of the propeller design for the Reynolds number:

- No correction;
- Correction according to Oostervald and Oossanen;
- ITTC78 correction.

The user is also able to specify:

- Twin screw - check this option if the ship has twin screws, otherwise the ship is assumed to have a single screw.

- Controllable pitch propeller / Noise reduced - checking one or both of these options applies a correction to the standard series propeller efficiency to account for noise reduced and/or controllable pitch designs. The correction made is as follows:

$$\eta_{0Corercted} = \eta_{0Series} \times correction \qquad \text{Eq. 12}$$

Where, correction is:
0.97 for noise reduced or controllable pitch;
0.94 for both noise reduced and controllable pitch.

The propeller optimization process checks the design against cavitation. To achieve this, the user has to enter a value of Shaft Height from which the cavitations' number is calculated. By interpolating the Burrill 5% cavitation line with this value of cavitation number, a minimum allowable value of blade area ratio is obtained. Hydro then ensures that the actual blade area ratio is greater than the minimum allowable value multiplied by the user specified cavitation safety factor. The actual BAR must also be greater than the user specified minimum Blade Area Ratio. Note that the propeller series data is limited by a minimum BAR of 0.4.
The input data are presented in Table 16 and the obtained results are depicted in Table 17.

Table 16. Given KCS propeller particulars.

Wageningen B-Series propeller		
Fixed Pitch		
Non-noise Reduced		
Efficiency factor	1.000	
Shaft height	4.000	metres
Cavitation SF	1.000	
Design speed	24.000	knots
Diameter	7.900	metres
Number of blades	5	
Min. Effective BAR	0.700	
Number of screws	1	
Reynolds number correction using ITTC method		

Table 17. Optimum propeller.

Diameter	7.900	metres
Pitch ratio	1.035	
Effective BAR	0.917	(0.917 min)
Local Cavitation no	0.362	
Thrust load. coeff.	0.146	(0.146 max)
Kt/J^2	0.535	
Adv. coeff. J	0.656	
Thrust coeff. Kt	0.230	
Torque coeff. Kq	0.0395	
Open water eff.	0.610	

The advance coefficient *J* of the optimum propeller can be calculated by the formulae:

$$J = \frac{V_A}{n * D} \rightarrow n = \frac{V_A}{J * D} \qquad \text{Eq. 13}$$

where D is the propeller diameter.

The advance speed V_A is determined from the wake fraction *w* and the ship speed:

$$V_A = V(1-w) \qquad \text{Eq. 14}$$

$$V_A = 24 * 0.5144 * (1 - 0.304)$$

$$V_A = 8.5925 m/s$$

The revolution rate of the propeller is:

$$n = \frac{8.5925}{0.656 * 7.9} = 1.658 rps$$

$$n = 99.5 RPM$$

The open water characteristics of a propeller, K_T (thrust coefficient), K_Q (torque coefficient), η_0 (open water efficiency) are given in Table 18 and are usually plotted in function of J (advance coefficient), see Figure 12.

Table 18. Kt - Kq Curves (open water characteristics.)

J	Kt	Kq	eta0
0.326	0.391	0.0620	0.327
0.390	0.362	0.0580	0.388
0.455	0.332	0.0537	0.447
0.519	0.300	0.0493	0.503
0.584	0.268	0.0447	0.556
0.648	0.234	0.0400	0.605
0.713	0.200	0.0352	0.646
0.777	0.166	0.0303	0.677
0.842	0.131	0.0253	0.692
0.906	0.095	0.0203	0.678
0.971	0.060	0.0153	0.608
1.035	0.025	0.0103	0.397

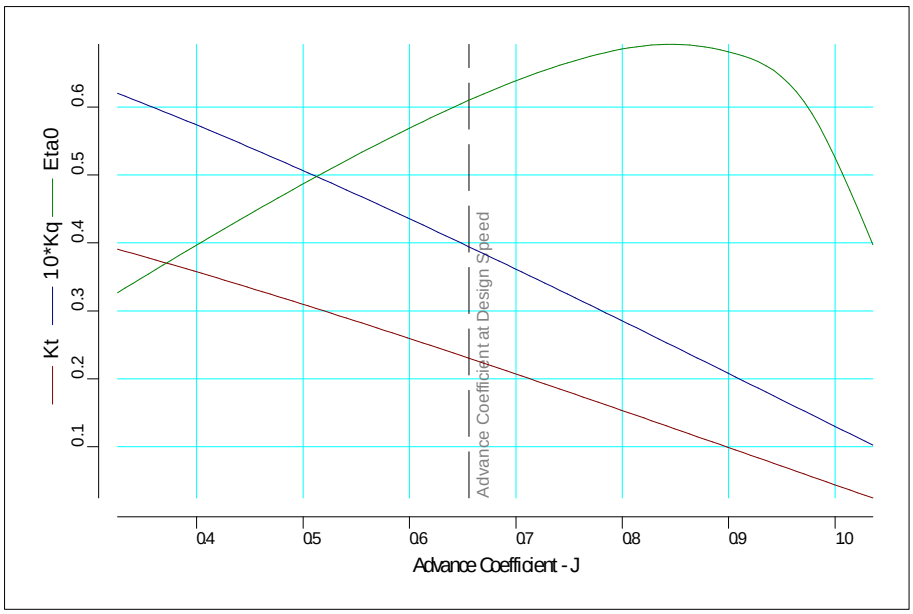

Figure 12. Open water characteristics of the optimum propeller.

2.4.3 Brake power

The main function of any propulsive system is to deliver thrust (power) to drive the ship forward at a designed speed. The speed-power prediction given by Powering module is presented in Table 18, where the *transmission efficiency* was equal with 0.97:

Pe – effective power;

THDF – thrust deduction fraction;

WFT – wake fraction;

ETAR – relative rotative efficiency;

ETA0 – open water efficiency;

QPC – quasi-propulsive coefficient;

Ps – brake power;

RPM – propeller revolution.

Table 19. Speed - Power results.

Speed kts	Pe (kW)	THDF	WFT	ETAR	ETA0	QPC	Ps (kW)	RPM
14.000	3899	0.195	0.306	0.988	0.638	0.732	5491	54.21
15.000	4814	0.195	0.306	0.988	0.638	0.731	6787	58.15
16.000	5892	0.195	0.306	0.988	0.637	0.730	8323	62.19
17.000	7164	0.195	0.305	0.988	0.636	0.728	10148	66.33
18.000	8664	0.195	0.305	0.988	0.634	0.725	12319	70.61
19.000	10435	0.195	0.305	0.988	0.631	0.722	14906	75.03

Speed kts	Pe (kW)	THDF	WFT	ETAR	ETA0	QPC	Ps (kW)	RPM
20.000	12528	0.195	0.305	0.988	0.628	0.718	17998	79.62
21.000	14975	0.195	0.304	0.988	0.624	0.713	21652	84.35
22.000	17801	0.195	0.304	0.988	0.620	0.708	25909	89.19
23.000	21116	0.195	0.304	0.988	0.615	0.703	30970	94.22
24.000	25135	0.195	0.304	0.988	0.610	0.696	37217	99.58
25.000	30003	0.195	0.304	0.988	0.603	0.688	44947	105.35
26.000	35604	0.195	0.303	0.988	0.595	0.680	54018	111.38

Figure 13 presents the propeller revolution diagram and in Figure 14 is depicted the brake power diagram given by powering module.

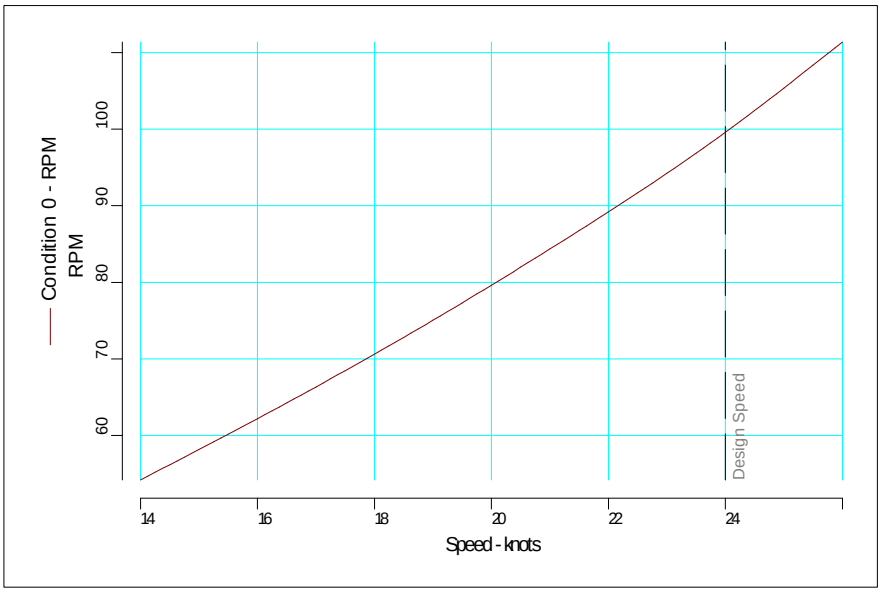

Figure 13. Propeller rotation speed diagram.

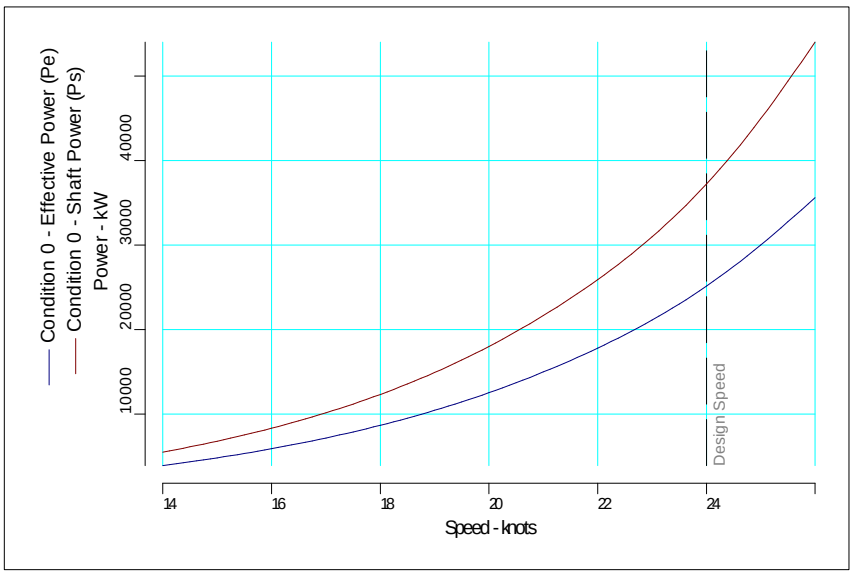

Figure 14. Brake power diagram.

The brake power is calculated by Tribon software without using any design and service margin. So, we have to calculate the brake power with the *power design margin* M_D and *power service margin* M_S contributions.

Effective power:

$$P_E = R_t * v * (1 + M_D) \qquad \text{Eq. 15}$$

$\boldsymbol{M_D}$ is *power design margin* (related to the predicted resistance). The usual values are:

M_D=0,01... 0.02, prediction based on the self-propulsion test with final propeller in the towing tank;

M_D=0,03... 0.06, prediction based on the self-propulsion test with stock propeller in the towing tank;

M_D=0,07... 0.08, prediction based on the resistance test in the towing tank;

M_D=0,10 , for preliminary theoretical prognosis (Holtrop-Mennen ,Guldhammer-Harvald, Taylor, SSPA, etc.).

Using the relation (15), the effective power is obtained:

$$P_E = 2035.469 * 12.35 * (1 + 0.10)$$
$$P_E = 27651.846KW$$

Delivered power:

$$P_D = \frac{P_E}{\eta_D * n_p} \qquad \text{Eq. 16}$$

Where $\boldsymbol{n_p}$ is the propellers number and η_D =QPC is the quasi-propulsive coefficient.

$$P_D = \frac{27651.846}{0.696 * 1}$$
$$P_D = 39729.664KW$$

Brake power at full rating (100 % MCR) is determined with following relation:

$$P_B = \frac{P_D}{\eta_{ax} * \eta_r * (1 - M_s)} \qquad \text{Eq. 17}$$

Where:

- $\boldsymbol{\eta_{ax}}$ **= *0.9***7, the line shaft bearing efficiency (equal with transmission efficiency used in powering module);
- $\boldsymbol{\eta_r = 1}$ (without gear reduction);
- $\boldsymbol{M_S}$**= *0.15 … 0.25***, power service margin in order to include the added power needed in service to overcome the added resistance from hull fouling, waves, wind, shallow water effects, etc. If the value M_S=0.225 is adopted, than the brake power is

$P_B = 52781.46KW$

Brake power at service rating (90 % MCR):

Brake power at service rating is determined by relation:

$$P_B^{SR} = \frac{P_B}{SR} \qquad \text{Eq. 18}$$

Where SR is the service rating of the main engine (85%-95%). If the value SR=0.9 is adopted, than the brake power at service rating will be

$$P_B^{SR} = \frac{52781.46}{0.9}$$

$$P_B^{SR} = 58646.06KW$$

2.5 Manoeuvring performances

The Manoeuvring module uses semi-empirical formulae for both merchant vessels and warships. This module can be used for prediction of the following ship manoeuvring characteristics: turning circle, zig-zag, crash stop and reverse spiral manoeuvres.

The manoeuvring calculations are based on mathematical models derived from regression analysis of data sets of manoeuvring characteristics.

In this case the sub-module had been used to predict the turning circle manoeuvre, zig-zag and reverse spiral manoeuvres characteristics.

The estimation had been made for deep water condition, at 18 knots.

The data summary is in the following Tables 20-21-22-23-24-25-36.

Table 20. General ship information.

Ship	KCS	
Vessel type	Merchant	
Condition	New	
Length	230.000	metres
Beam	32.200	metres
Mean Draught	10.8000	metres
Trim	0.0000	metres
Block coef.	0.6560	
LCG from Aft Perp.	111.2470	metres
Bulb present		

Table 21. Rudder information.

No. of Rudders	1	
Height	9.900	metres
Area	54.450	sq.metres

No. of Rudders	1	
Aspect ratio	1.800	
Turn rate	2.140	
Type	Conventional	
Distance from midship	115.000	metres
Distance to load waterline	1.000	metres

Table 22. Propeller information.

No. of Propellers	1	
No. of blades	5	
Diameter	7.900	metres
Mean Pitch	8.177	metres
Blade Area Ratio	0.917	

Table 23. Engine properties.

Astern Stopping Power	2000.000	kW
Approach Speed	18.000	knots

Table 24. Non-Dimensional hydrodynamic coefficients (calculated).

Yv	-1283.750	Nv	-487.937		
Yr	282.343	Nr	-204.567		
Yvd	-789.451	Nvd	N/A		
Yrd	N/A	Nrd	-41.515		
Stabd	-0.33337				
Xrr	N/A	Yr|r|	240.610	Nr|r|	-109.822
Xvv	N/A	Yv|v|	-2287.410	Nrrv	138.015
Xvr	527.432	Yr|v|	1347.930	Nvvr	-753.602

Table 25. Resistance coefficients. (All values multiplied by 10e-5) .

AD1	7434.747
AD2	-926.182
AD3	133.601

Table 26. Propulsion point at manoeuvring speed, using BSRA Series.

Wake fraction	0.305	
Thrust Deduction fraction	0.195	
Ship Speed	18.00	knots
Propeller RPM	70.66	
Total Ship Resistance	957.680	kN

2.5.1 Mathematical model

One of the general models is the Abkowitz nonlinear model for ship manoeuvring, which contain the equations of free motion of a body in six degrees of freedom:

We consider a rigid body dynamics, with a right-handed direction coordinate system fixed on the body, Oxyz:

- the origin Oxyz fixed at midship section ;

- the longitudinal x-axis, is situated in the centreline plane, parallel to the still water plane positive forward ;

- the transversal y-axis, is perpendicular to the plane of symmetry positive to starboard

- the vertical z-axis, is perpendicular to the still water plane positive downward.

Figure 15 depicts the coordinate system of the ship.

We consider the following notations:

δ is rudder angle;

β is drift angle of the ship;

ψ is the heading angle;

u and v are ship speed in x-axis and y-axis respectively, with the corresponding acceleration $\dot{u}$, $\dot{v}$ and r is angular speed.

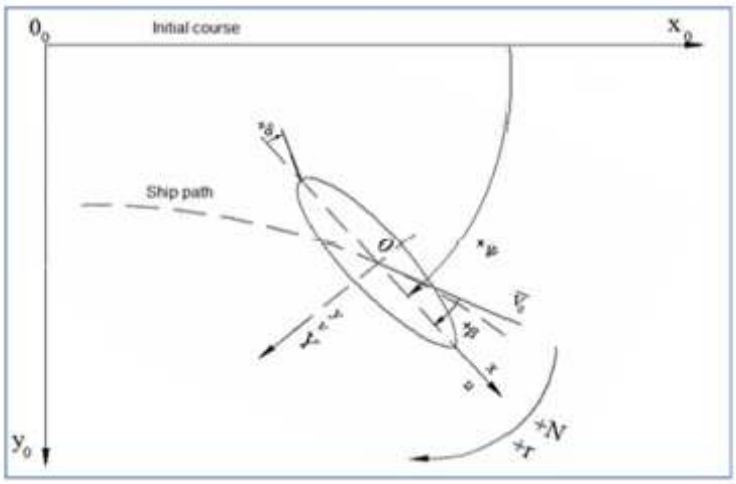

Figure 15. Coordinate system of ship.

For analysing the ship motions with six degrees of freedom, two theorems can be used:

- the linear momentum theorem :

$$\sum_{i=1}^{N} \overline{F}_i = \sum_{i=1}^{N} \frac{d}{dt}(m_i * \overline{v}_i) \qquad \text{Eq. 19}$$

where m is the mass of the small particle i, F_i is the external force acting on the particle i and v_i is the speed.

- the angular momentum theorem :

$$\sum_{i=1}^{N} (\overline{M}_i + \overline{r}_i + \overline{F}_i) = \sum_{i=1}^{N} \overline{r}_i * \frac{d}{dt}(m_i * \overline{v}_i) \qquad \text{Eq. 20}$$

where :

r_i : the referenced radius vector;

M_i : the external moment which act on the particle i.

If we consider at the origin the ship speed is $\bar{v}_0$ and the angular speed is $\bar{\omega}$, so the total speed will have this expression:

$$\bar{v}_i = \bar{v}_0 + \bar{\omega} * \bar{r}_i \qquad \text{Eq. 21}$$

By replacing the equation 21 of total speed in equation 19 we get

$$\sum_{i=1}^{N} \bar{F}_i = \sum_{i=1}^{N} \frac{d}{dt}(m_i * (\bar{v}_0 + \bar{\omega} * \bar{r}_i)) = m * \frac{\partial \bar{v}_0}{\partial t} + \frac{d}{dx}\left(\bar{\omega} * \sum_{i=1}^{N} m_i * \bar{r}_i\right) \qquad \text{Eq. 22}$$

If we consider the total mass $m = \sum_{i=1}^{N} m_i$, and the vector of centre of gravity $\bar{r}_G$ we note:

$$m * \bar{r}_G = \sum_{i=1}^{N} (m_i * \bar{r}_i) \qquad \text{Eq. 23}$$

In this model these conventions are used:

$$\begin{aligned} \bar{r}_G &= x_G * \bar{i} + y_G * \bar{j} + z_G * \bar{k} \\ \bar{v}_0 &= u * \bar{i} + v * \bar{j} + w * \bar{k} \\ \bar{\omega} &= p * \bar{i} + q * \bar{j} + r * \bar{k} \\ \bar{F} &= X * \bar{i} + Y * \bar{j} + N * \bar{k} \end{aligned} \qquad \text{Eq. 24}$$

The linear momentum is given by the following formula ($\bar{r}_G \neq 0$)

$$\begin{aligned} X &= m\left[\frac{\partial u}{\partial t} + qw - rv + \frac{dq}{dt} z_G - \frac{dr}{dt} y_G + (qy_G + rz_G)p - (q^2 + r^2)x_G\right] \\ Y &= m\left[\frac{\partial v}{\partial t} + ru - pw + \frac{dr}{dt} x_G - \frac{dp}{dt} z_G + (rz_G + px_G)q - (r^2 + p^2)y_G\right] \\ Z &= m\left[\frac{\partial w}{\partial t} + pv - qu + \frac{dp}{dt} y_G - \frac{dq}{dt} x_G + (px_G + qy_G)r - (p^2 + q^2)z_G\right] \end{aligned} \qquad \text{Eq. 25}$$

The different moments of inertia are presented by:

$$I = \begin{vmatrix} I_{xx} & I_{xy} & I_{xz} \\ I_{yx} & I_{yy} & I_{yz} \\ I_{zx} & I_{zy} & I_{zz} \end{vmatrix} \quad \begin{aligned} I_{xx} &= \sum_{i=1}^{N} m_i (y_i^2 + z_i^2) \\ I_{yy} &= \sum_{i=1}^{N} m_i (x_i^2 + z_i^2) \\ I_{zz} &= \sum_{i=1}^{N} m_i (y_i^2 + x_i^2) \\ I_{xy} = I_{yx} &= \sum_{i=1}^{N} m_i x_i y_i) \\ I_{xz} = I_{zx} &= \sum_{i=1}^{N} m_i x_i z_i) \\ I_{yz} = I_{zy} &= \sum_{i=1}^{N} m_i y_i z_i) \end{aligned} \qquad \text{Eq. 26}$$

The same procedures are applied for the angular momentum theorem and we obtained the following motion:

$$K = \frac{\partial p}{\partial t} I_{xx} + \frac{\partial q}{\partial t} I_{xy} + \frac{\partial r}{\partial t} I_{xz} + rq(I_{zz} - I_{yy}) + (q^2 - r^2) I_{yz} + pqI_{xz} - prI_{xy} + m\left[y_G (\frac{\partial w}{\partial t} + pv - qu) - z_G (\frac{\partial v}{\partial t} + ru - pw) \right] \qquad \text{Eq. 27}$$

$$M = \frac{\partial p}{\partial t} I_{yx} + \frac{\partial q}{\partial t} I_{yy} + \frac{\partial r}{\partial t} I_{yz} + pq(I_{xx} - I_{zz}) + (r^2 - p^2) I_{xz} + qrI_{xy} - qpI_{yz} + m\left[z_G (\frac{\partial u}{\partial t} + qw - rv) - x_G (\frac{\partial w}{\partial t} + pv - qu) \right] \qquad \text{Eq. 28}$$

$$N = \frac{\partial p}{\partial t} I_{zx} + \frac{\partial q}{\partial t} I_{zy} + \frac{\partial r}{\partial t} I_{zz} + pq(I_{yy} - I_{xx}) + (p^2 - q^2) I_{xy} + prI_{yz} - qrI_{xz} + m\left[x_G (\frac{\partial v}{\partial t} + ru - pw) - y_G (\frac{\partial u}{\partial t} + qw - rv) \right] \qquad \text{Eq. 29}$$

By considering $\bar{r}_G = 0$, and if we neglect the cross-inertia terms in the plane x-y, the equations of motions become:

$$\begin{aligned} X &= m\left(\frac{\partial u}{\partial t} + qw - rv \right) \\ Y &= m\left(\frac{\partial v}{\partial t} + ru - pw \right) \\ N &= \frac{\partial r}{\partial t} I_{zz} + pq(I_{yy} - I_{xx}) \end{aligned} \qquad \text{Eq. 30}$$

By considering $\bar{r}_G \neq 0$, and knowing that the ship is symmetric we get $y_G = 0$, $w = 0$, $q = 0$ and also by neglecting the roll motion which means $p = 0$ and $K = 0$, so the equations of motion become:

$$X = m\left(\frac{\partial u}{\partial t} - rv - r^2 x_G\right)$$
$$Y = m\left(\frac{\partial v}{\partial t} + ru + \frac{dr}{dt} x_G\right) \qquad \text{Eq. 31}$$
$$N = \frac{\partial r}{\partial t} I_{zz} + m x_G \left(\frac{\partial v}{\partial t} + ru\right)$$

Where:

X,Y: represent the hydrodynamic forces respectively (surge, sway).

N: the vertical hydrodynamic moment (yaw moment)

2.5.2 Turning circle manoeuvre

The turning circle is defined by the rudder angle, equal with 35° and a direction of the motion (starboard or portside) with all previous mentioned data. The summary of the turning circle are presented in table 26 and the output results are in Tables 27-28 and Figures 16 and 17. *The KCS has very good manoeuvring abilities*.

Table 27. Summary of the turning test.

Ship name	KCS	
Loading Condition	New	
Approach Speed	18.000	knots
Rudder Command Angle	35.000	deg.
Water depth	Deep	

Table 28. Output results of the turning test

ADVANCE/L	AT 90 DEG	3.35	
TRANSFER/L	AT 90 DEG	1.88	
SPEED/APR. SPEED	AT 90 DEG	0.71	
TIME	AT 90 DEG	122.00	SECS
MAX ADVANCE/L	AT 90 DEG	3.38	
MAX TRANSFER/L	AT 90 DEG	2.21	
TACTICAL DIAM/L		3.96	
ADVANCE/L	AT 180 DEGS	1.96	
SPEED/APR. SPEED	AT 180 DEGS	0.56	
TIME	AT 180 DEGS	234.00	SECS
MAX TACTICAL DIAM/L		3.99	

ADVANCE/L	AT 90 DEG	3.35	
MAX ADVANCE/L	AT 180 DEGS	1.65	
TRANSFER/L	AT 270 DEGS	2.75	
ADVANCE/L	AT 270 DEGS	0.12	
SPEED/APR. SPEED	AT 270 DEGS	0.50	
TIME	AT 270 DEGS	348.00	SECS
STEADY TURNING DIAM/L		2.85	
STEADY TURNING RATE		0.76	DEG/S
NON DIM. TURNING RATE (L/R)		0.70	
TRANSFER/L	AT 360 DEGS	1.03	
ADVANCE/L	AT 360 DEGS	1.27	
STEADY DRIFT ANGLE		11.55	DEGS
SPEED/APR. SPEED	AT 360 DEGS	0.47	
TIME	AT 360 DEGS	466.00	SECS

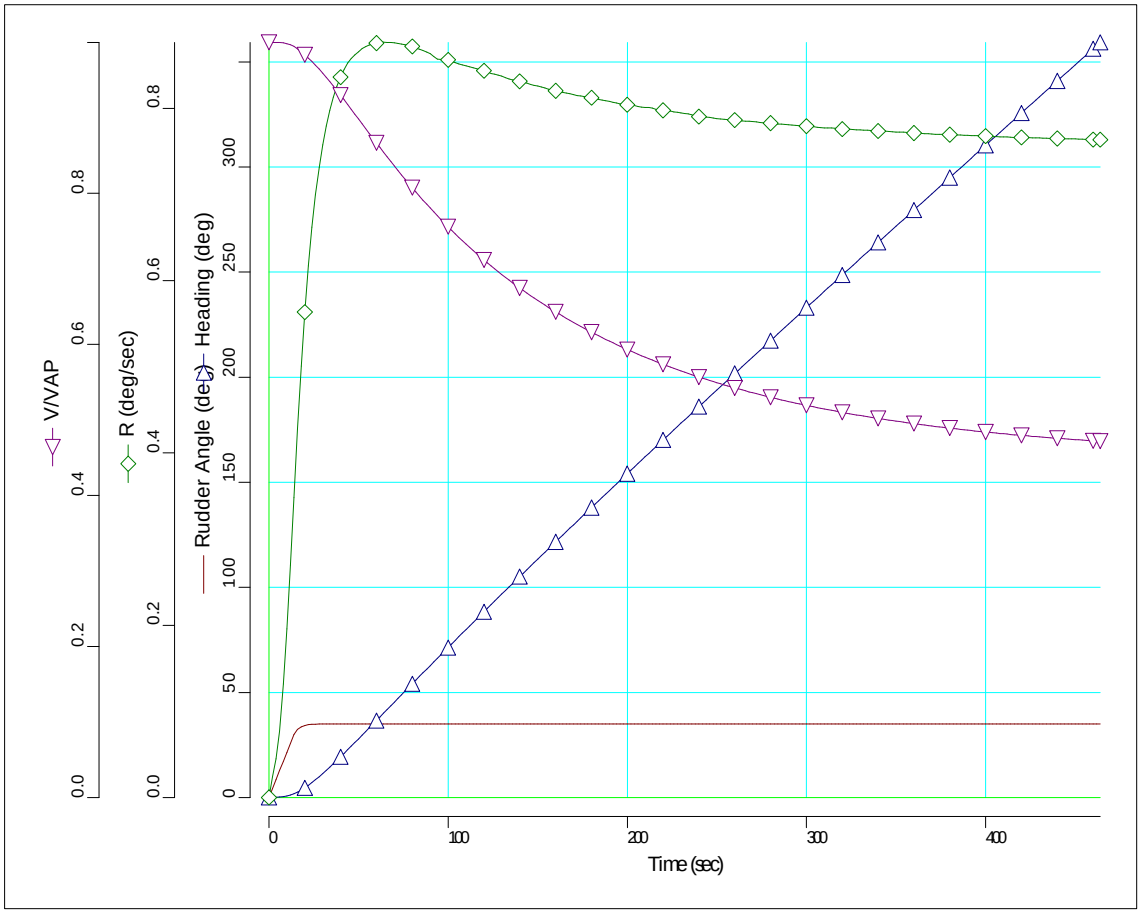

Figure 16. Turning characteristics of the ship in deep water

2.5.3 Zig-Zag Manoeuvre

In zig-zag manoeuvres we initiate test to starboard by giving rudder angle 10° at first execute, then it is alternatively shifted to portside after the ship reached 10° in second execute, and keep changing for followings. The turning abilities (K) and quick response indexes (T) are presented in Table 29. The output results of zig-zag manoeuvres are presented in Table 30 and Figures 17-18. *The small values of the overshoot angles suggest very good counter-manoeuvring abilities.*

Table 29 .First Order Steering Quality Indices K & T.

Ship name	KCS	
Loading Condition	New	
Type of zig-zag Manoeuvre (Rudder/Check)	10.0 / 10.0	
Approach speed	18.000	knots
Residual Helm Angle	0.271	deg
Turning Ability Index (K)	0.044	1/sec
Non-dimensional Turning Ability Index	1.101	
Quick Response Index (T)	32.775	sec.
Non-dimensional Quick Response Index (T)	1.320	
R.M.S. Yaw rate	0.313	deg/s
Non-dimensional R.M.S. Yaw rate	0.135	

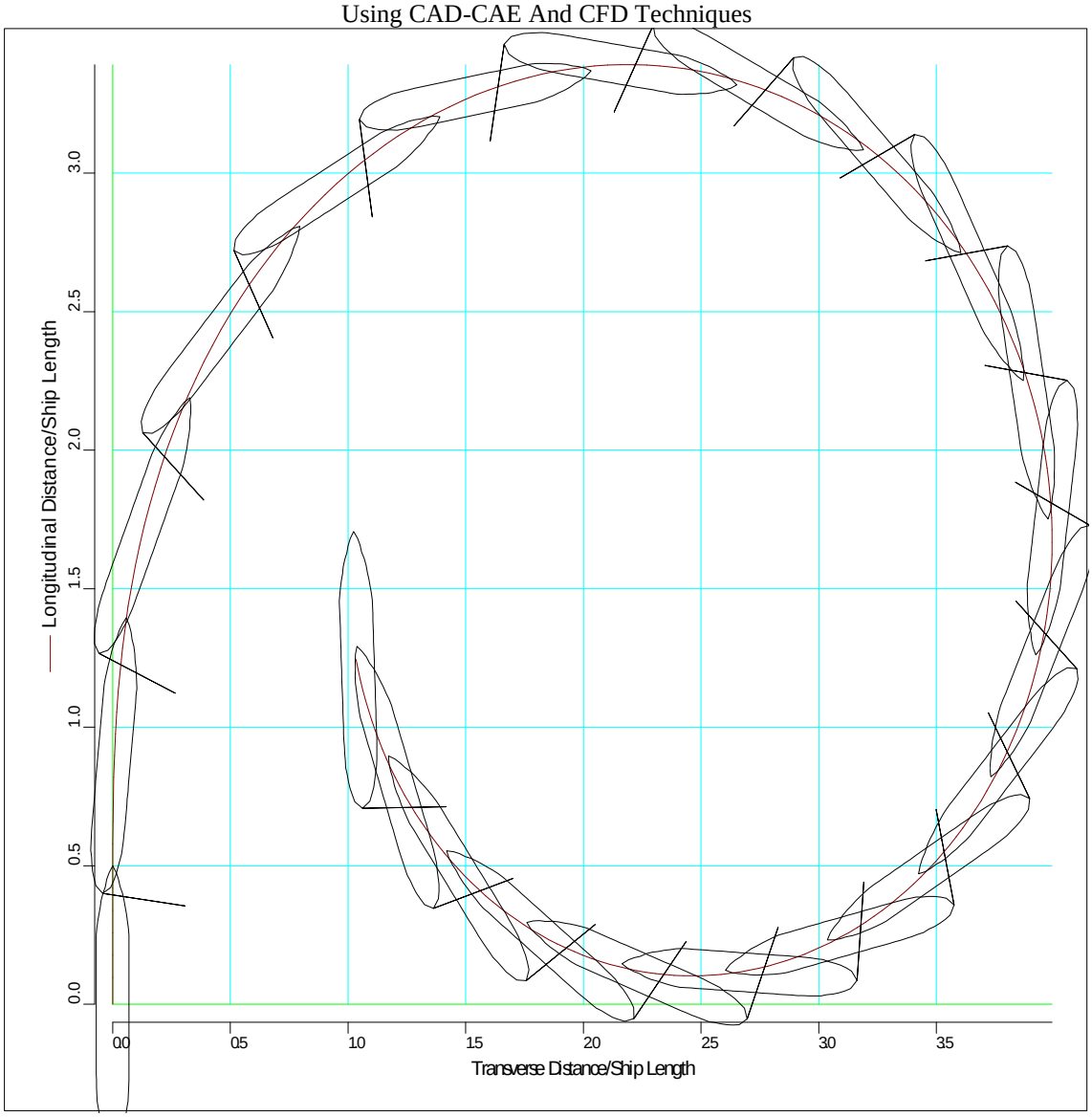

Figure 17. Turning trajectory of the ship in deep water.

Table 30. Summary of Zig-Zag Manoeuvre.

Ship name	KCS	
Loading Condition	New	
Approach Speed	18.000	knots
Rudder Command Angle	10.000	deg.
Heading Check Angle	10.000	deg.
Water depth	Deep	

1ST OVERSHOOT ANGLE	6.50	DEG
1ST OVERSWING ANGLE	4.14	DEG
2ND OVERSHOOT ANGLE	7.38	DEG
2ND OVERSWING ANGLE	4.91	DEG
3RD OVERSHOOT ANGLE	6.74	DEG
3RD OVERSWING ANGLE	4.22	DEG

1ST OVERSHOOT ANGLE	6.50	DEG
4TH OVERSHOOT ANGLE	6.50	DEG
4TH OVERSWING ANGLE	4.43	DEG
PERIOD	226.00	SEC
INITIAL TURNING TIME	44.00	SEC
1ST TIME TO CHECK YAW	24.00	SEC
1ST LAG TIME	19.33	SEC
2ND TIME TO CHECK YAW	26.00	SEC
2ND LAG TIME	21.33	SEC
3RD TIME TO CHECK YAW	24.00	SEC
3RD LAG TIME	19.33	SEC
4TH TIME TO CHECK YAW	24.00	SEC
4TH LAG TIME	19.33	SEC
OVERSHOOT WIDTH OF PATH/LENGTH	0.69	

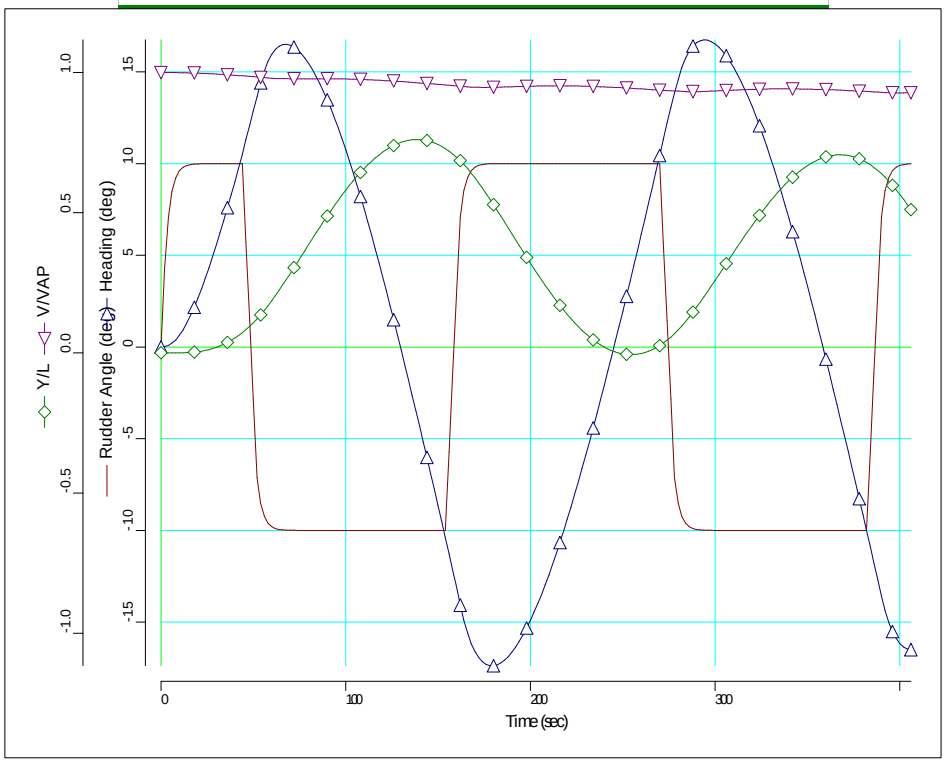

Figure 18. Zig-Zag Characteristics of the Ship in Deep water.

2.5.4 Spiral Manoeuvre

The performance of spiral manoeuvre provides and checks the directional stability of the KCS ship. The results are presented by the yaw (rate of turn) vs. the rudder angle diagram, for both sides starboard and port.

To start the spiral test the rudder is deflected by 35° for starboard and held till the rate of change heading will be constant. Then the rudder angle is decreased by 5°, till it reached to 0°. Then same procedure is done for the port side by increasing the rudder angle. The summary of the reverse spiral manoeuvre is presented in table 30 and the output results in Tables 31-32-33 and Figures 19-20. *The KCS is stable on route because of the straightness of the red curve* (without the hysteresis curve).

Table 31 .Summary of Reverse Spiral Manoeuvre.

Ship name	KCS	
Loading Condition	New	
Approach Speed	18.000	knots
Water depth	Deep	

Table 32. Reverse Spiral Values : Starboard Rudder Angles.

Rudder Angle deg	Yaw Rate deg/sec	Yaw Rate Non. Dim	Ship Speed/Approach Speed
0.00	0.00	0.00	1.00
1.33	0.10	0.04	1.00
3.06	0.20	0.09	0.98
5.20	0.29	0.13	0.94
7.74	0.38	0.18	0.90
10.75	0.46	0.24	0.85
15.00	0.56	0.31	0.77
20.00	0.64	0.40	0.69
25.00	0.70	0.50	0.61
30.00	0.74	0.60	0.53
35.00	0.76	0.70	0.47

Table 33. Reverse Spiral Values : Port Rudder Angles.

Rudder Angle deg	Yaw Rate deg/sec	Yaw Rate Non. Dim	Ship Speed/Approach Speed
0.00	-0.00	-0.00	1.00
-1.37	-0.10	-0.04	1.00
-3.12	-0.20	-0.09	0.98
-5.26	-0.30	-0.13	0.95
-7.81	-0.39	-0.18	0.91
-10.78	-0.47	-0.24	0.85

Rudder Angle deg	Yaw Rate deg/sec	Yaw Rate Non. Dim	Ship Speed/Approach Speed
-15.00	-0.57	-0.32	0.77
-20.00	-0.66	-0.42	0.68
-25.00	-0.72	-0.53	0.60
-30.00	-0.76	-0.64	0.52
-35.00	-0.79	-0.75	0.45

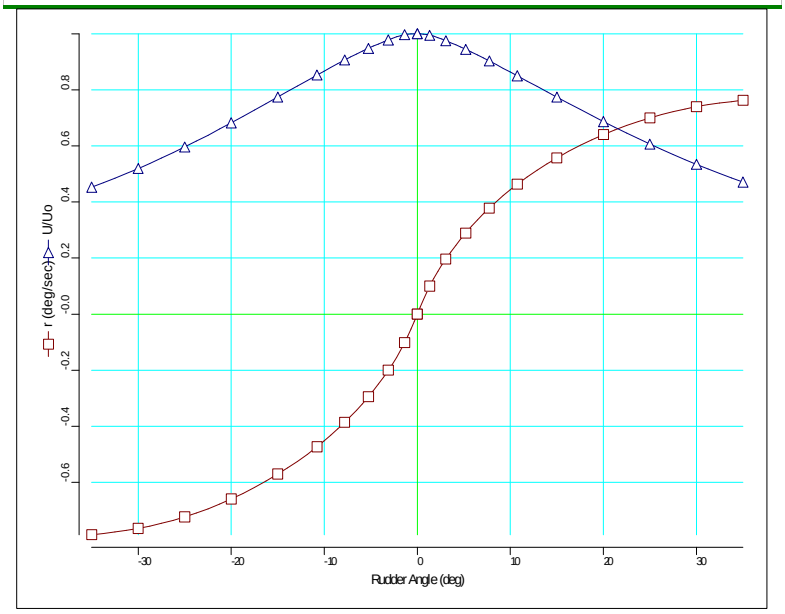

Figure 19 . (Dimensional) Reverse Spiral Manoeuvre of the Ship in Deep water.

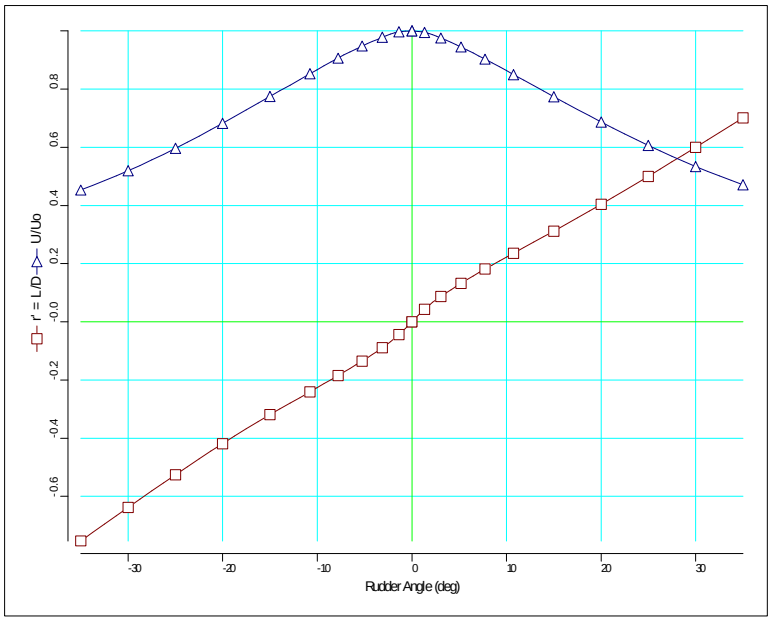

Figure 20. (Non-Dimensional) Reverse Spiral Manoeuvre of the Ship in Deep water.

Ship manoeuvrability standards are developed for traditional ships with traditional propulsion system.

The International Maritime Organization updates these standards periodically and are applied for all types of propulsion and rudder systems, of ships from 100 m length and above.

The following Table 34 resume the IMO rules compared to the results of the manoeuvring performances.

Table 34 IMO criteria for maneuvring performances.

STANDARD MANOEUVRE	MAXIMUM VALUES		KCS values
TURNING CIRCLE	Advance (AD)	≤ 4,5 *L*	3.35
	Tactical diameter (TD)	≤ 5 *L*	3.96
ZIG-ZAG MANOEUVRE	First overshoot angle (zigzag 10°/10°)	≤10° if *L/v*<10 sec.	6.5
		≤20° if *L/v*>30 sec.	
		≤ (5+0,5*L/v*) [degrees] if 10 sec.<*L/v*<30 sec.	
	Second overshoot angle (zig-zag 10°/10°)	Should not exceed the first overshoot angle by more than 15°	7.80
	First overshoot angle (zigzag 20°/20°)	≤25°	
CRASH- STOP	The track reach	≤15 *L*	

From these results and comparison with IMO rules we can say that the KCS hull has good manoeuvring performances.

3 CFD Analysis of the free surface potential flow around the KCS hull

Computational Fluid Dynamics has been progressed rapidly in past sixty years. Many industrial fields have used CFD and it plays an irreplaceable role for engineering design and also scientific research. Unfortunately, inherent the solutions from the CFD code has error or uncertainty in the results. In order to achieve the computational simulation full potential as a predictive tool, engineers must have confidence that the simulation results are an accurate representation of reality. Verification and validation provide a framework for building confidence in computational simulation predictions. The flow field of container ship KCS with free surface at full scale was simulated using the SHIPFLOW solver. The Korea Research Institute for Ships and Ocean Engineering (now MOERI) performed towing tank experiments to obtain resistance, mean flow data and free surface waves for KCS (Van et al [7], 1998, Kim et al [8], 2001). These results can be obtained from the web [1].

The free surface flow of a modern container ship KCS without propeller was firstly simulated using three sets of grids.

CFD analysis of the flow around the ship hull in SHIPFLOW is related to naval and marine applications, which is based on two approaches: Global and Zone approaches. The simulation in this thesis is based on the global approach. And to run SHIPFLOW two types of files are needed: offset file and command file, see Figure 21.

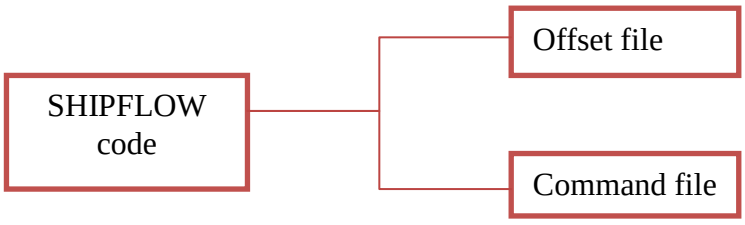

Figure 21. Workflow in shipflow code.

The offset file

The main purpose of an offset file is describing the geometry of the hull and it is done by giving a list of points. Each point is defined by its coordinates x, y and z. The stations are given by the intersection between a constant x plane and the hull. Also there are groups where each group describes the shape of a full part of the hull. Generally we have one group describing the main hull, the keel or the bossing, the bulb. For describing the main part of the hull, more than one group can be used, each one identified by a label name. In the same

manner, all points have a status flag that describe the way how to treat these points by the program (station's first point, station's points or end point of the group).

For KCS hull four groups have been created and are presented in the following Figure 22.

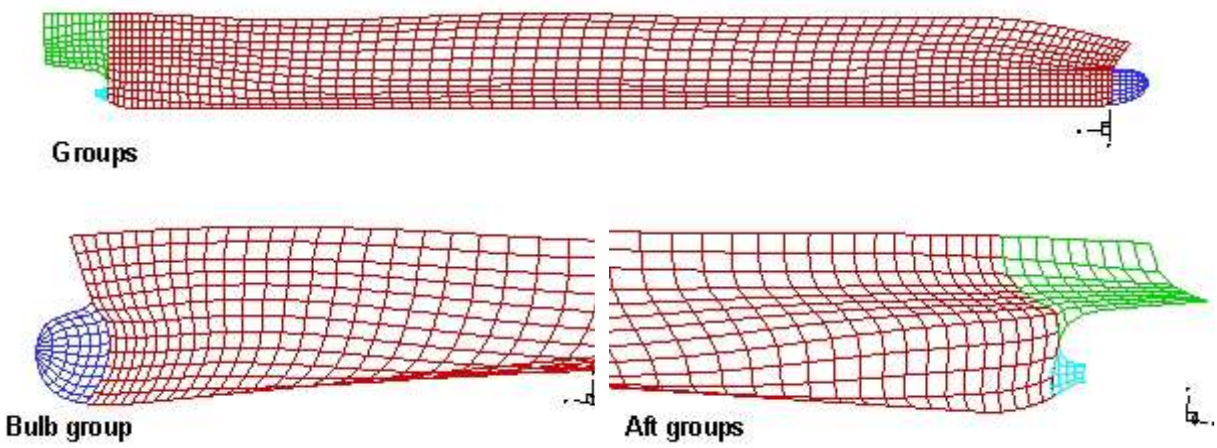

Figure 22. Different groups of the KCS hull.

The command file

The command file is a set of instruction for the code to run different modules and, in the meanwhile, to define all physical properties in the problem including: initial position, initial speed, type of the hull, propeller geometry, and symmetry also fluid characteristics. It contains:

1. The title
2. Information of programs and modules executed.
3. Name of the offset file with the definition of the coordinate system used and the groups in the offset file
4. Type of hull, length scale and ship speed.

The command file for SHIPFLOW is written with Notepad++.

The CFD process is developed in three steps pre-processing, processing and post-processing. For the pre-processing we use XMESH and XGRID modules. For the processing we use XPAN, XBOUND and XCHAP modules. Tecplot is used to visualize the output files (results).

The following Figure 23 presents the different process in SHIPFLOW.

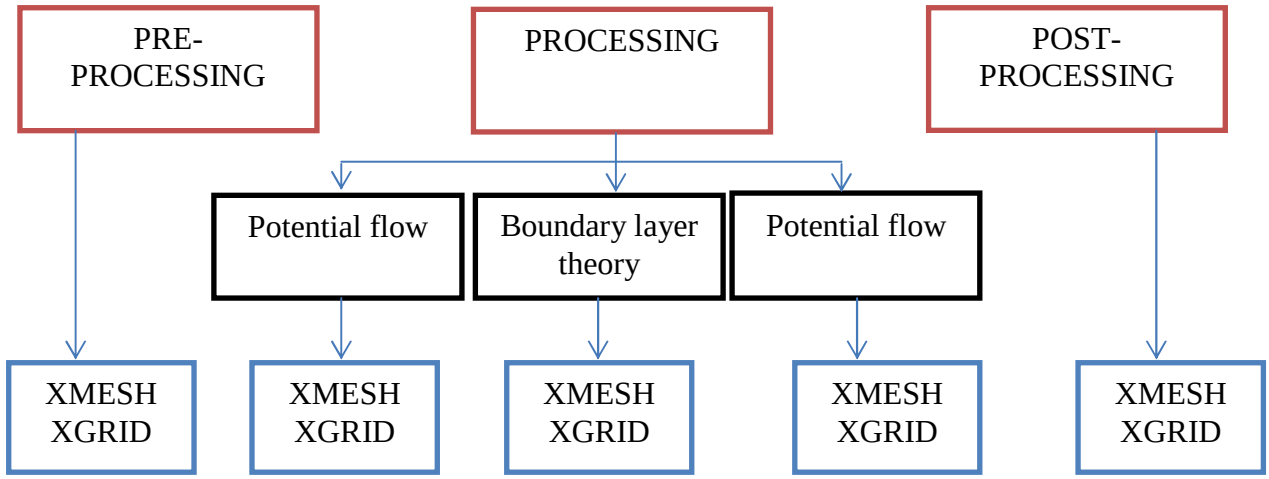

Figure 23. Different process in SHIPFLOW.

The methods used for computing the ship resistance computations:

XMESH is the mesh generator (panel generator) for the potential flow module XPAN

XPAN is the potential flow solver. The flow is solved around three dimensional bodies by using the mesh generated by XMESH module and also by using the surface singularity panel method. The free surface flows use non-linear free surface boundary condition.

XBOUND is a processing flow solver. It is a program for thin turbulent boundary layer computations and also used for the laminar and transition boundary layer computations.

3.1 Mathematical model, [4]

Basically, the algorithm follows the model previously proposed by Lungu and Raad [4]. Assuming steady, irrotational flow of an inviscid and uncompressible fluid, the problem of computing the free surface flow around the ship is reduced to that of satisfying Laplace equation for the velocity potential in the fluid domain subject to the boundary condition on the body and kinematic and dynamic boundary condition on the unknown free surface. Equation field and boundary conditions are expressed in terms of velocity potential. The coordinate system is defined to represent the flow patterns around the hull as positive x in the flow direction, positive y in the starboard, and positive z upward where the origin is at the bow and undisturbed free surface. The coordinate system has the same speed as the ship but does not follow the ship movements such trim and sink.

For an inviscid and irrotational flow, the velocity $\mathbf{V} = (u, v, w)$ can be expressed as a gradient of a scalar function named the velocity potential:

$$\mathbf{V} = \nabla\phi \qquad \text{Eq. 32}$$

The governing equation for the potential flow method is Laplace equation:

$$\nabla^2\phi = 0 \qquad \text{Eq. 33}$$

Linearization of Laplace equation offers the possibility to combine elementary solutions (sources, sinks, doublets) to arbitrarily complicated solutions. Thus we can consider the total velocity potential as a sum of double model velocity potential and the perturbation velocity potential due to presence of free surface:

$$\phi = \phi_0 + \phi_w \qquad \text{Eq. 34}$$

The potential is subject to the several conditions on the hull and free-surface boundaries. At infinity the velocity is supposed to be undisturbed:

$$\lim_{r\to\infty}|\nabla\phi| = 0 \qquad \text{Eq. 35}$$

Body boundary condition requires that no fluid particle penetrate the hull surface, therefore

$$\phi_n = 0 \qquad \text{Eq. 36}$$

The development of the free surface is governed by the kinematic and dynamic boundary conditions on the free surface. Kinematic boundary condition is the mathematical formulation of the physical condition that a particle at the surface should remain at the surface all the time:

$$\phi_x\zeta_x + \phi_y\zeta_y - \phi_z = 0 \text{ on } z = \zeta \qquad \text{Eq. 37}$$

The dynamic condition requires that the pressure on the free surface must be equal to the atmospheric pressure. Normally it could be set to zero. Dynamic boundary condition on the free surface is derived from Bernoulli equation and may be written as:

$$g\zeta + 0.5\cdot\left(\phi_x^2 + \phi_y^2 + \phi_z^2 - U_\infty^2\right) = 0 \text{ on } z = \zeta \qquad \text{Eq. 38}$$

The free-surface problem described above is difficult to solve since the free surface boundary conditions (6) and (7) are non-linear and must be satisfied on the initially unknown wavy surface. Dawson method [3], [5] is based on the double-model method which places a mirror image of the body to the undisturbed free surface. The free-surface condition is linearized in terms of the velocity potential of the double-model solution and it is satisfied by the addition

of a source density on the undisturbed free surface *z=0*. By substituting equation (7) into equation (6) one may get:

$$\varphi_x\left(\varphi_x^2+\varphi_y^2+\varphi_z^2\right)_x+\varphi_y\left(\varphi_x^2+\varphi_y^2+\varphi_z^2\right)_y+ \\ +2g\varphi_z=0 \qquad \text{Eq. 39}$$

Substituting equation (3) into equation (8) then assuming that (8) holds on *z=0* and neglecting the higher-order terms of the perturbation potential and its partial differentiation equation (8) becomes:

$$\varphi_{0l}^2\varphi_{wll}+2\varphi_{0l}\varphi_{0ll}\varphi_{wl}+g\varphi_{wz}=-\varphi_{0l}^2\varphi_{0ll} \qquad \text{Eq. 40}$$

where *l* is the streamline direction of the double model solution on the undisturbed free surface *z=0*.

Finally radiation condition is dealt with by the use of a four-point, upstream, finite difference operator for the free surface condition. Forces and moments, including wave resistance are computed by integrating pressure over the ship hull.

3.2 Panelization

In this study, three sets of refined grids were generated by XMESH module. Multiblock structured mesh has been used .

The calculations of the Reynolds number and the Froude number based on ship length and ship velocity may be seen in Table 35.

Table 35.Froude number and Reynolds number.

V (Knts)	V (m/s)	Fr	Re
14	7,2016	0,151611	1,59E+09
16	8,2304	0,1732697	1,81E+09
18	9,2592	0,1949284	2,04E+09
20	10,288	0,2165871	2,27E+09
22	11,3168	0,2382458	2,49E+09
24	12,3456	0,2599045	2,72E+09
26	13,3744	0,2815632	2,95E+09

The number of the stations and points created for the panelization are listed in Tables: 36-37-38 for all three sets of grids.

Coarse:

For the coarse mesh generated, the number of panels is 2608, with a number of nodes of 2838. Below, Table 36 defines the stations and points for each group.

Table 36. Stations and points for coarse mesh

	stations	points
hull	72	11
bulb	7	11
bulbstern	10	7
overhang	5	5

The Figures 24-25 represent the coarse mesh on the KCS hull and on the free surface.

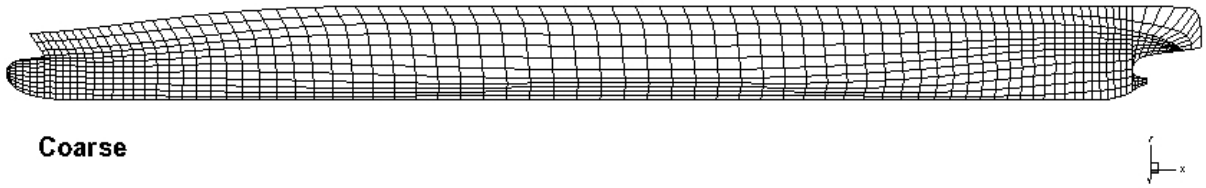

Figure 24. Coarse mesh on the KCS hull.

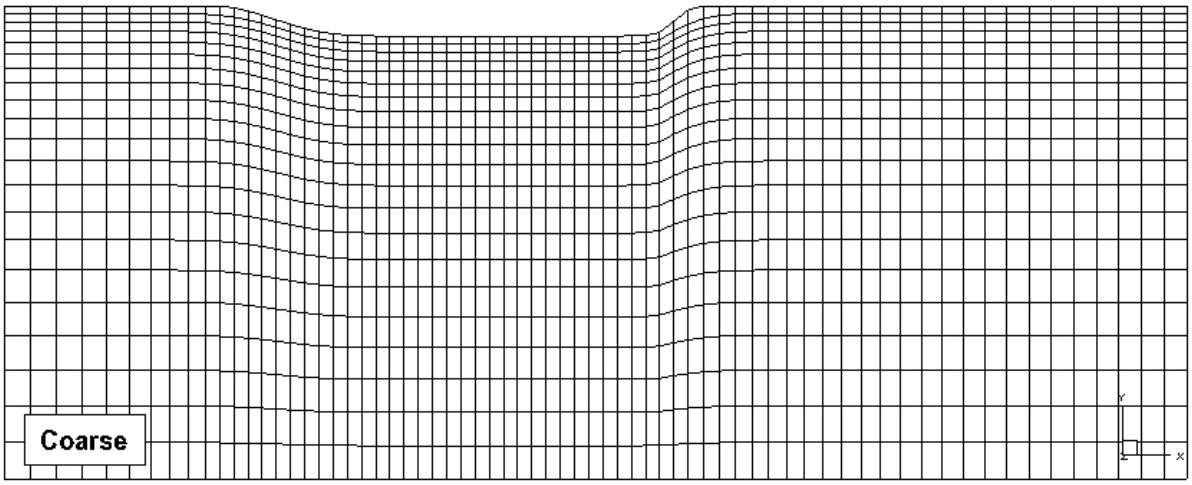

Figure 25. Coarse mesh on the free surface.

Medium

For the medium mesh generated, the number of panels is 6568, with a number of nodes of 6930. Table 37 defines the stations and points for each group.

Table 37. Stations and points for medium mesh.

	stations	points
hull	115	17
bulb	12	17
bulb stern	16	12
overhang	5	8

The Figures 26-27 represent respectively the coarse mesh on the KCS hull and on the free surface.

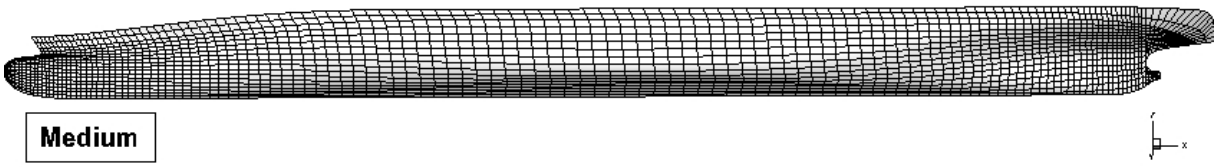

Figure 26. Medium mesh on the KVS hull.

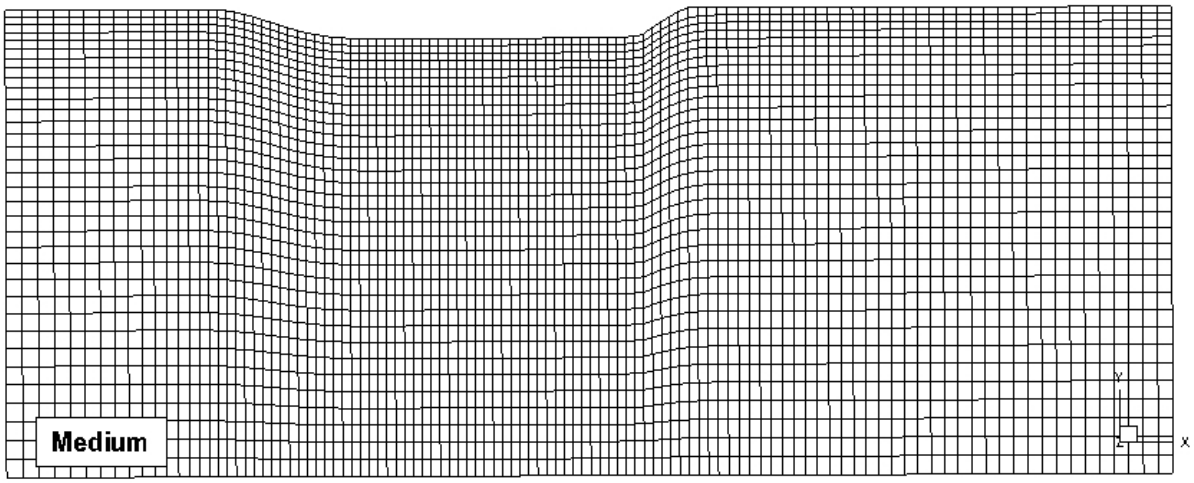

Figure 27. Medium mesh on the free surface.

Fine

For the medium mesh generated, the number of panels is 10458, with a number of nodes of 10912. Table 38 defines the stations and points for each group.

Table 38. Stations and points for Fine mesh.

	stations	points
hull	144	22
bulb	15	22
bulb stern	20	15
overhang	5	10

The Figures 28-29 represent respectively the coarse mesh on the KCS hull and on the free surface.

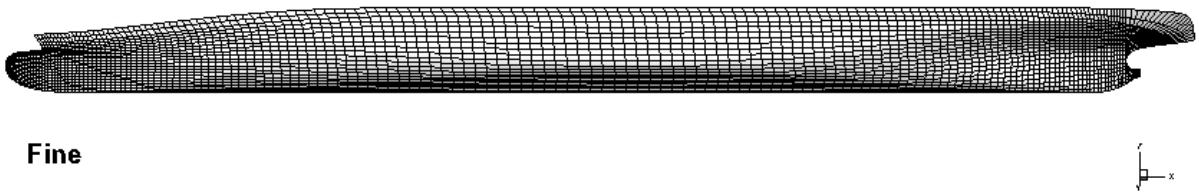

Figure 28. Fine mesh on the KCS hull.

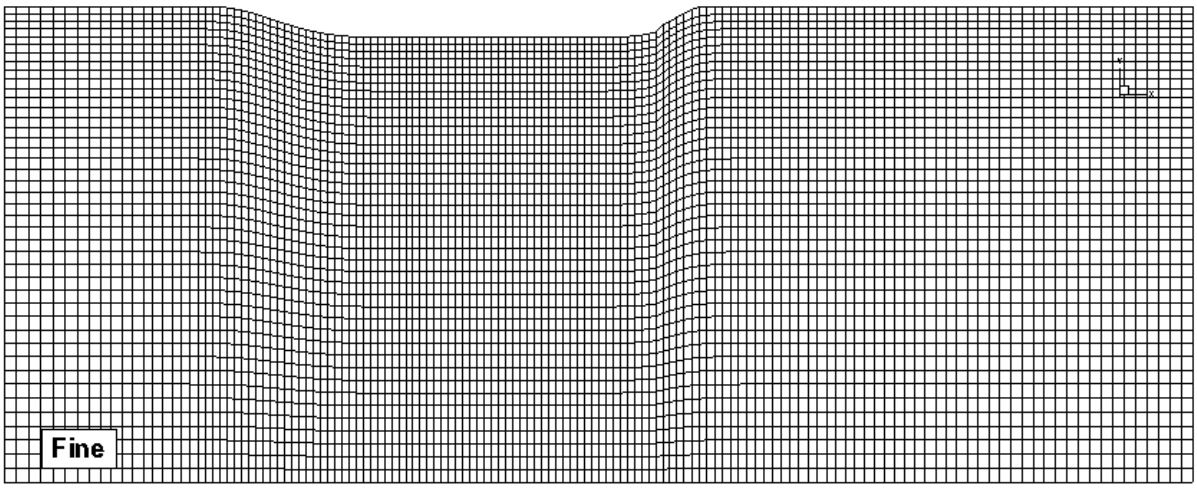

Figure 29. Fine mesh on the free surface.

3.3 Free surface potential flow simulation

The modules used for free surface potential flow simulation are XPAN and XBOUND (boundary layer theory). The calculation was attained at full scale for length of Lpp= 230 m. and draught T=10.8 m for a range of speeds [14 Knots – 26 Knots].

Hydrodynamic parameters which can be solved by the potential flow theory are: the pressure contour on the ship hull, wave profile (wave cut), free surface, wave pattern.

The free surface flow around the KCS hull is carried by a 7 sets of non-linear computations, which also calculate the ship resistance coefficients.

3.3.1 Free surface

The free surface potential flow of the KCS hull at design speed is presented in the Figures 30-31-32 for different sets of grids.

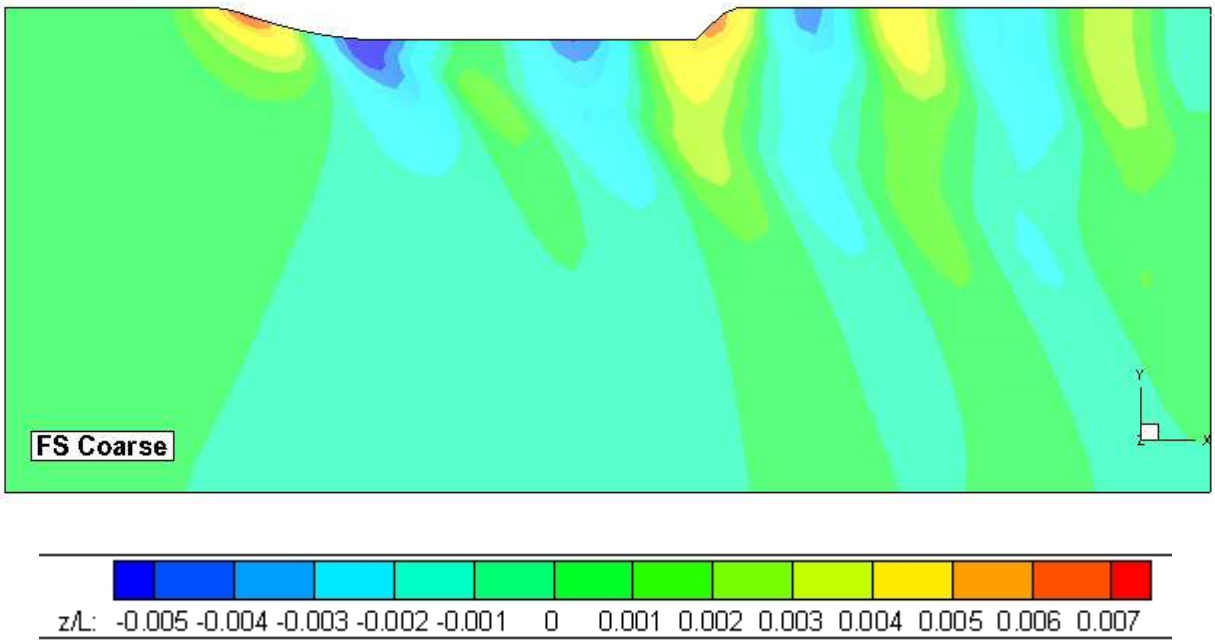

Figure 30. Free surface potential flow at 24 Knts speed for coarse mesh.

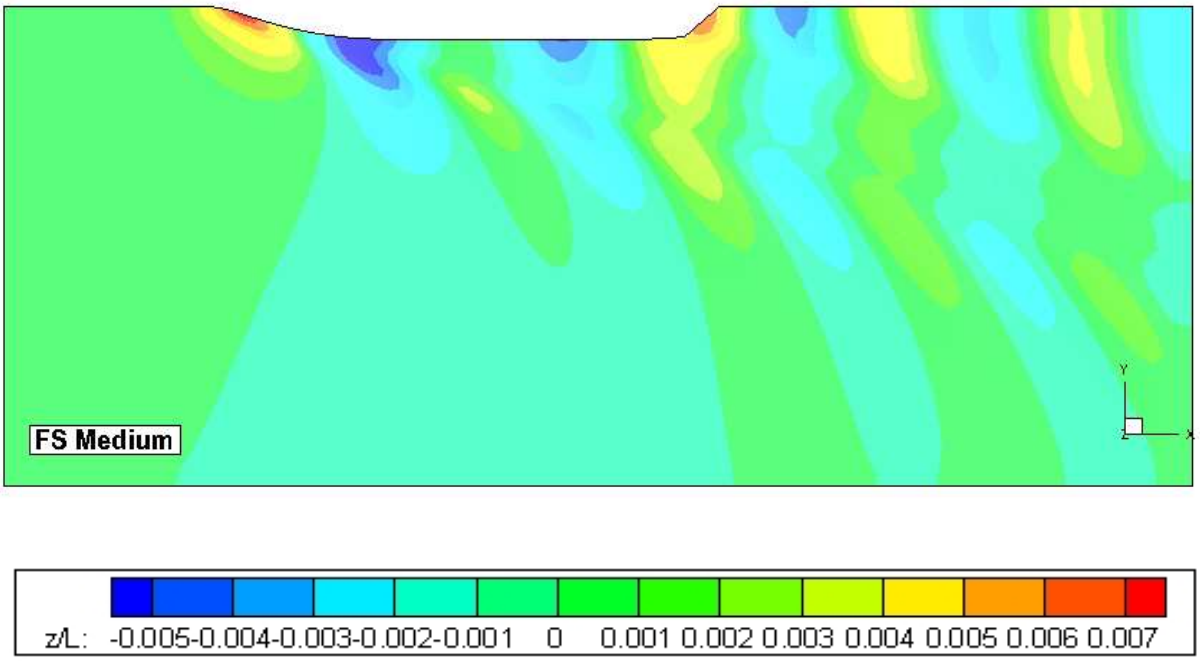

Figure 31. Free surface potential flow at 24 Knts for medium mesh.

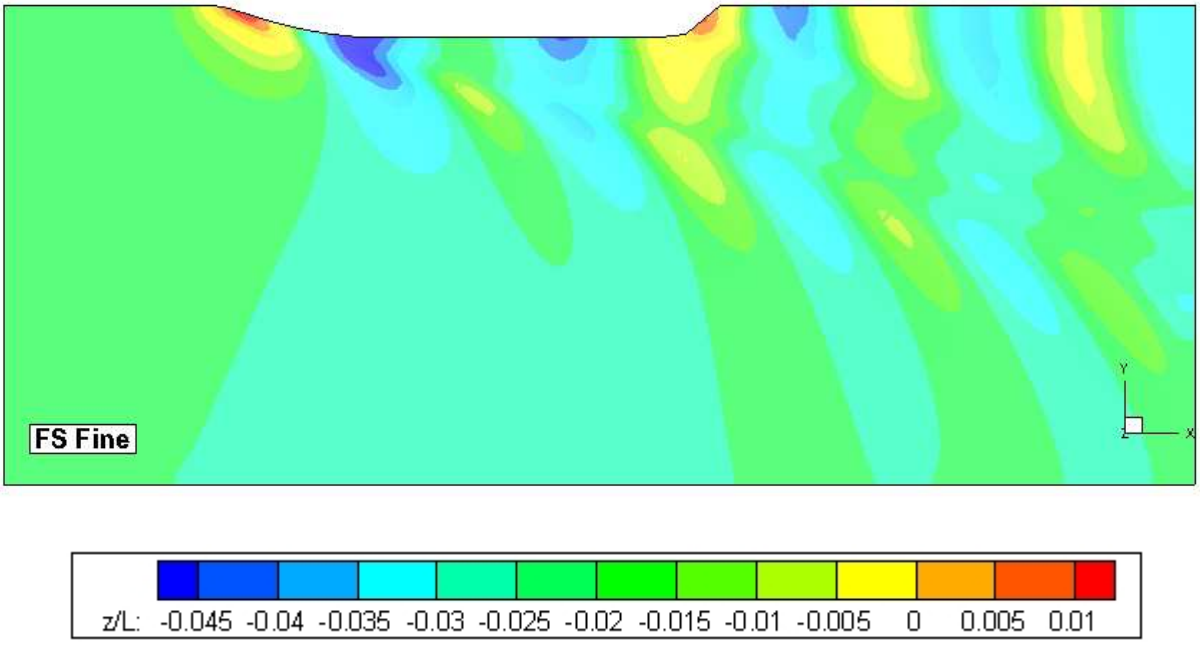

Figure 32. Free surface potential flow at 24 Knts for fine mesh.

3.3.2 Pressure on the body

The pressure contours around the KCS hull for the designed speed 24 Knots, and for three sets of mesh are presented in the Figures 33-34-35.

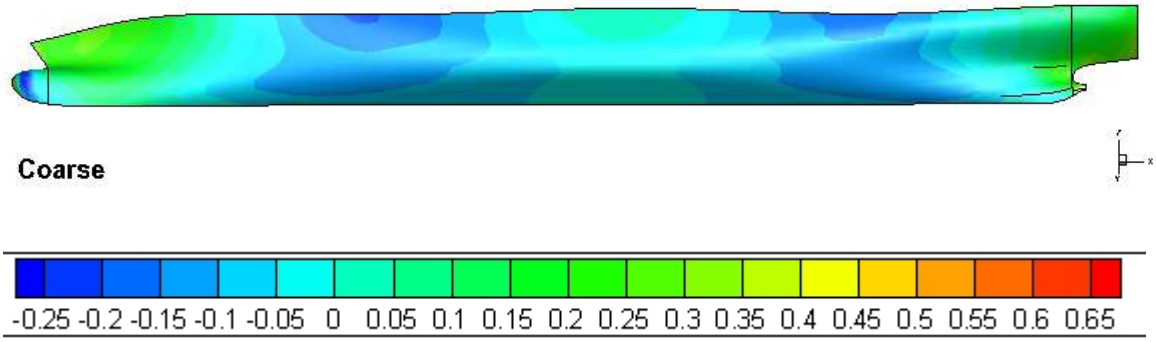

Figure 33. Pressure field on the KCS body at 24 Knts for coarse mesh.

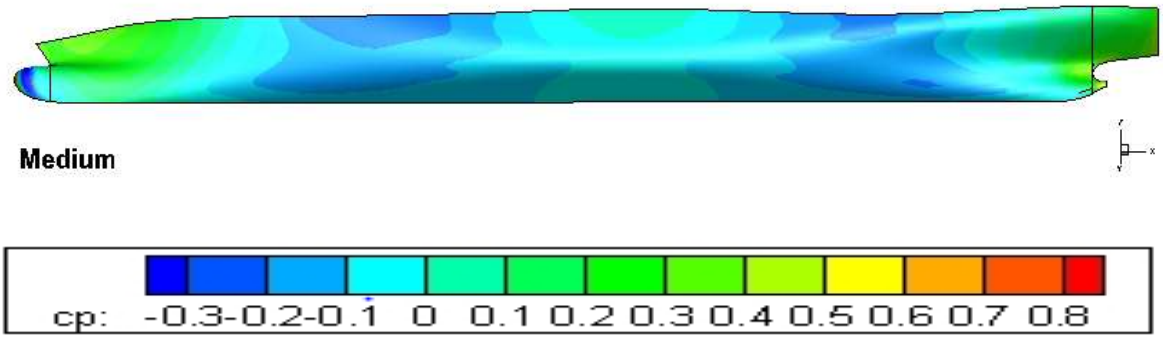

Figure 34. Pressure field on the KCS body at 24 Knts for medium mesh.

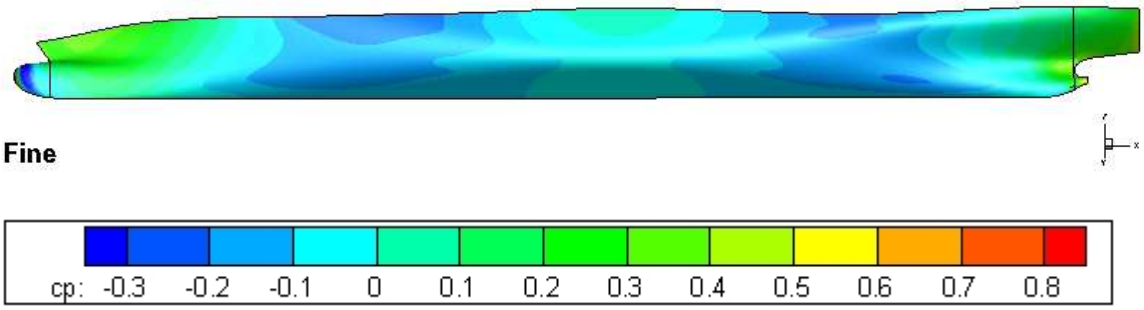

Figure 35. Pressure field on the KCS body at 24 Knts for fine mesh.

3.3.3 Wave elevation

The advance of ship in calm water generates waves on the free surface, the wave profile of the KCS hull is presented in the Figure 36 at the design seed 24 Knots with a comparison of three sets of grid.

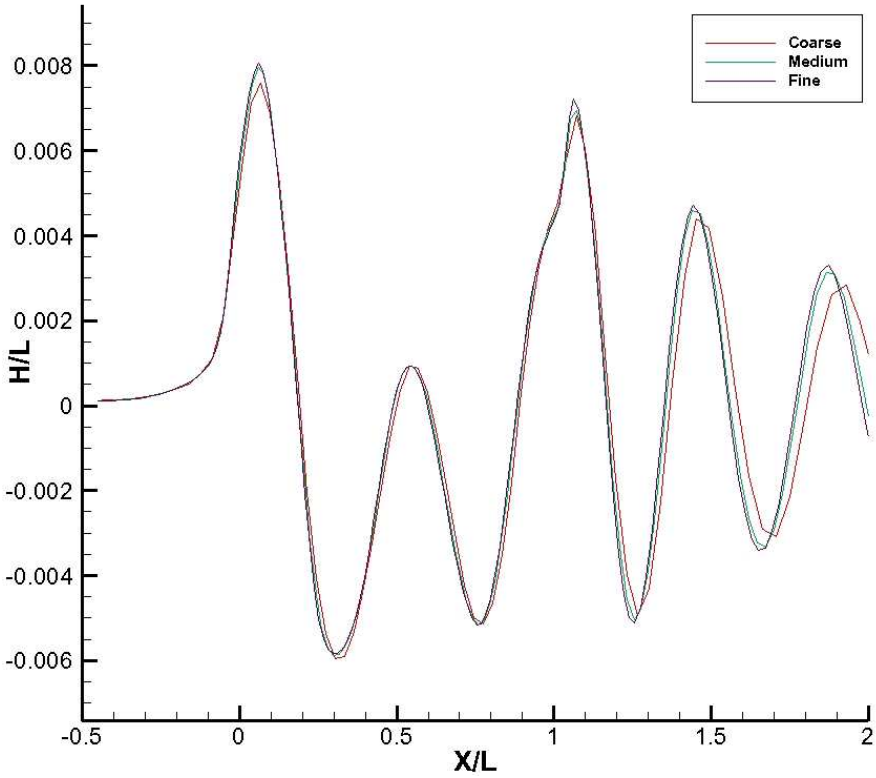

Figure 36. Wave profile on the waterline for 24 Knts speed.

From this figure one can see that the wave elevation for the coarse mesh has less amplitude the two others meshes medium and fine.

3.3.4 Resistance

The total resistance was calculated by the same module and the results are presented in Figure 37.

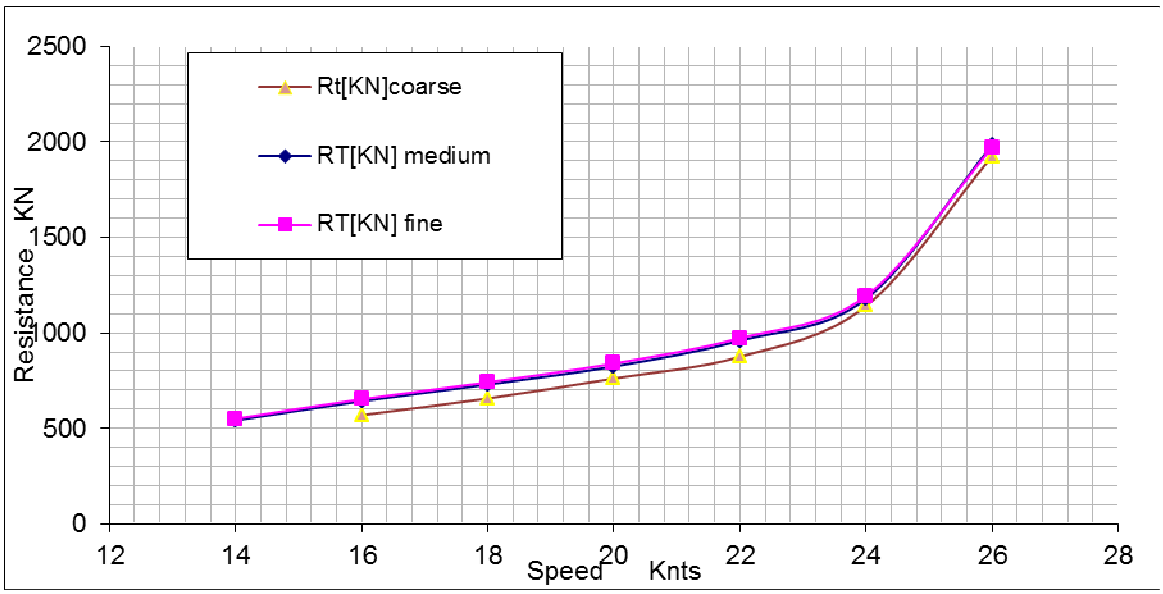

Figure 37. Resistance of the KCS hull for three sets of grid.

From this figure one can observe that the medium and refined mesh gives more closed results than the coarse mesh. And the following Table 39 gives comparison of Fine mesh with both coarse and medium

Table 39. Comparison of resistance results bitween different meshes.

v[kn]	%(fine/medium)	%(fine/coarse)
14	1,501803	-
16	1,593875	14,60752
18	1,565562	12,84336
20	1,886173	10,34025
22	1,315562	11,09756
24	1,211897	4,554813
26	-0,62007	2,395019

From this table one can observe that the difference between the medium and the fine mesh results are less than 2%, while the difference between the fine and coarse mesh is about 9.3%.

4 CFD Analysis of the viscous flow around the KCS hull

4.1 Mathematical model, [14]

In fluid dynamics the equations of continuity, energy and momentum are fundamental; also known that the Navier-Stokes equations are the most used in viscous flow calculations. Here is a brief description of the mathematical model and formulations suitable for viscous flow free surface simulations.

4.1.1 Flow equations

The Navier-Stokes equations describe the aero and hydrodynamics of the ship. These equations are obtained by applying Newton's second law to an element of fluid and is assumed that the viscous stress is proportional to the strain rate. However, it cannot solve the Navier-Stokes equations for cases of a very practical interest because they contain small scales to solve them.

These equations can be time averaged, Larsson and Raven (2010), Reynolds stresses are introduced as new unknowns for removing turbulence scales from the simulations. we call the time averaged equations : Reynolds-averaged Navier-Stokes, RANS, equations. For resolving Reynolds stresses separate equations are required.

In the continuous domain the fluid will be modelled as a mixture of two fluids water and air so for both the same equations are used for modelling. We consider the gravity as the only force which act the particle and is vertically directed along the *z,* axis upwards, the incompressible steady state, RANS equations will be in a component form as follow:

$$\frac{\partial}{\partial x}(\rho u^2 + p) + \frac{\partial}{\partial y}(\rho uv) + \frac{\partial}{\partial z}(\rho uw) = (\frac{\partial \tau_{xx}}{\partial x} + \frac{\partial \tau_{xy}}{\partial y} + \frac{\partial \tau_{xz}}{\partial z})$$
$$\frac{\partial}{\partial x}(\rho uv) + \frac{\partial}{\partial y}(\rho v^2 + p) + \frac{\partial}{\partial z}(\rho uw) = (\frac{\partial \tau_{yx}}{\partial x} + \frac{\partial \tau_{yy}}{\partial y} + \frac{\partial \tau_{yz}}{\partial z}) \qquad \text{Eq. 41}$$
$$\frac{\partial}{\partial x}(\rho uw) + \frac{\partial}{\partial y}(\rho vw) + \frac{\partial}{\partial z}(\rho w^2 + p) = (\frac{\partial \tau_{zx}}{\partial x} + \frac{\partial \tau_{zy}}{\partial y} + \frac{\partial \tau_{zz}}{\partial z}) - \rho g$$

Where:

u,v,w: velocity components.

p: the mean pressure + $\frac{2}{3}\rho k$.

ρ : the density.

g: the acceleration of gravity.

τ_{ij} : stress tensor defined by:

$$\tau_{ij} = (\mu + \mu_T)(\frac{\partial u_i}{\partial x_j} + \frac{\partial u_j}{\partial x_i}) \quad \text{Eq. 42}$$

Where:

μ : Dynamic viscosity

μ_T : Turbulent dynamic viscosity.

k: turbulent kinetic energy.

The flow is solved in two fluid domain both water and air. The density and the dynamic viscosity are discontinuous in the interface between pure water and pure air.

The equation of continuity solves the RANS equations, by the theorem of the conservative transport of mass. Which is described by the fact of that total mass transport in a system should be zero whiteout including any source. The equations are as follow for the fluids considered incompressible:

$$\frac{\partial u}{\partial x} + \frac{\partial v}{\partial y} + \frac{\partial w}{\partial z} = 0 \quad \text{Eq. 43}$$

4.1.2 Interface capturing method

In continuous domain for two incompressible fluids, the formulations Eq41 and Eq43 allow to solve the problem for a variable density, with an additional water fraction α to the equations of conservation of momentum and mass, the transport equation is given which has been derived from the mass conservation theorem equation for the water fluid only.

$$\frac{\partial}{\partial x}(\alpha u) + \frac{\partial}{\partial y}(\alpha v) + \frac{\partial}{\partial z}(\alpha w) = 0 \quad \text{Eq. 44}$$

α : [0-1]: the amount of water in the mixture

We consider the dynamic viscosity and density for the pure fluids as constants (incompressible fluid) however in the fluid mixture it varies in the domain. Therefore the dynamic viscosity and the density are proportional at each location to the water fraction α :

$$\mu = \alpha\mu_w + (1-\alpha)\mu_a$$
$$\rho = \alpha\rho_w + (1-\alpha)\rho_a$$ Eq. 45

4.1.3 Turbulence model

The turbulence model Menter $k-\omega SST$, Menter (1993), is used in this implementation for computing μ_T. This model is valid to the solid walls, so there will be no need for any wall function. The free surface interface is free with no treatment. Both good properties of the $k-\omega$ model near the wall and $k-\varepsilon$ outside of this region are combined in the $k-\omega SST$ by using the switching functions or the blending.

4.1.4 Boundary conditions

Two of the basic and appropriate boundary conditions used, Neumann and Dirichlet, are necessary for solving the system of equations. The first one determines the values of the normal derivatives to a surface solution and the second one determines the value of the domain boundary solution, these conditions are used differently according to the type of boundaries with each physical properties that are defining any computational problem, Versteg and Malalasekra (1995).

Inlet. We assume the flow is undisturbed. The velocity and the turbulent quantities are constant values. The Dirichlet BC describes the void fraction. But it varies at the inlet face, and takes values equal to 0 in the air and 1 in the water. In the longitudinal direction the pressure gradient is equal to zero.

Outlet. We take the boundary far downstream as simplification, this means that entire damping is posed to the waved and the flow is fully developed. With this assumption it will be acceptable that the Neumann boundary condition is used for the void fraction, for the velocity and also for the turbulent quantities. For this surface capturing method the Neumann boundary condition is also implemented for the pressure.

Slip. The domain in which we place the hull is assumed to have the physical boundaries like sides, bottom and top as solid walls. The flow in such a boundary condition is not ensured (the component of normal velocity is assumed to be zero) and free slip condition of the flow along the boundaries (the gradient of normal velocity is also zero). We use the Neumann boundary condition for the void fraction, pressure and turbulent quantities. These conditions are also used at the plane of symmetry. And also it is good assumption for the outer boundary if the

ship dimensions are small compared to the computational domain. For the top of the boundary we can apply a modified slip condition to solve the pressure equation the Dirichlet boundary condition is used.

Noslip. The velocity is assumed to be zero at the hull surface i.e. the fluid will stick to the surface and no possible flow through the boundary. The Neumann boundary condition will be used for void fraction and the pressure.

Here in Figure 38 is presented the Volume fraction plotted for the KCS hull .

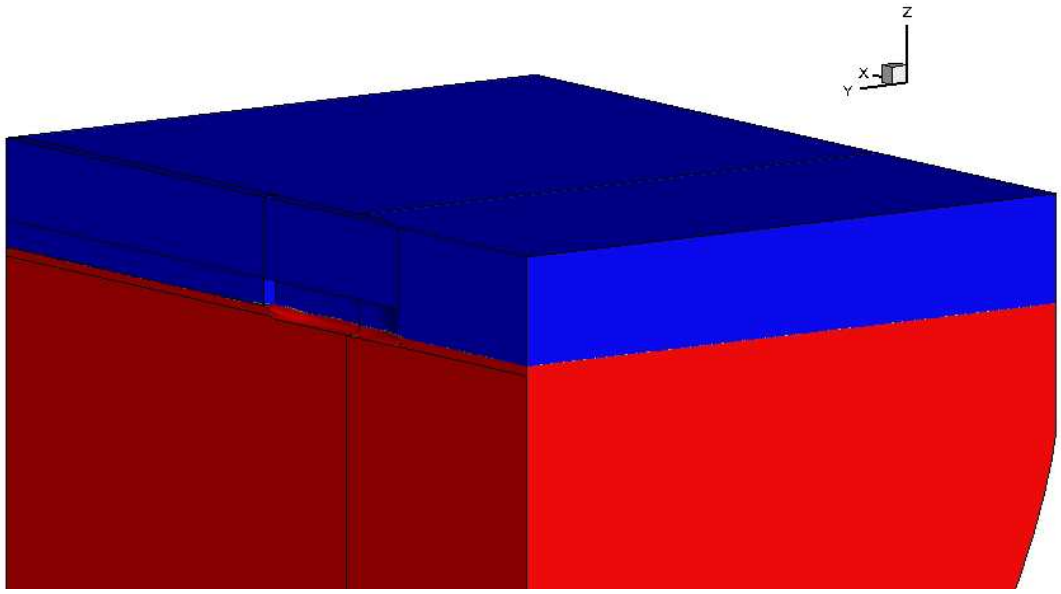

Figure 38. Volume fraction.

4.2 Computational grid

The Finite Volume Method (FVM) discretizes the partial differential equations to algebraic equations. From the face flux we can calculate in each cell volume the averaged values. This method is conservative however the flux which enters a volume through a face is equals to the flux which is leaving the adjacent volume through the same face. the Figures 39-40 present the 3D grids on the VOF.

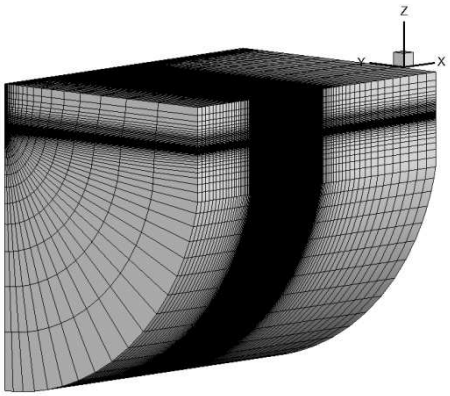

Figure 39. The 3D grid for the viscous flow.

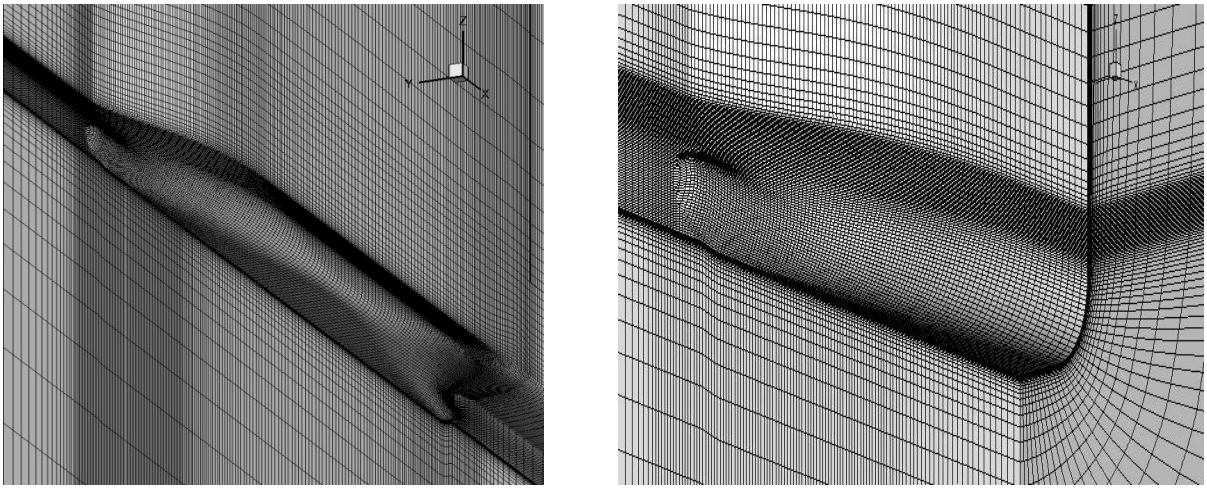

Figure 40. Coarse mesh on the KCS hull for viscous flow.

The total number of cells on the coarse grid for viscous flow calculation is 2300157 for all ship speeds [14 Knots – 24 Knots].

4.3 Viscous flow simulation

In the RANS solver in SHIPFLOW, XCHAP module have been used for the simulation of the viscous flow around the KCS ship hull, only the coarse mesh has been applied to the ship KCS hull, we could not apply all the meshes (medium and fine) because of the high need for processors which the computers in the lab cannot support.

The following characteristics as free surface around the hull and pressure distribution on the body, also the total resistance are obtained for different speeds, and in the following Figures 41-42-43 are presented the results obtained for the designed speed 24 Knots.

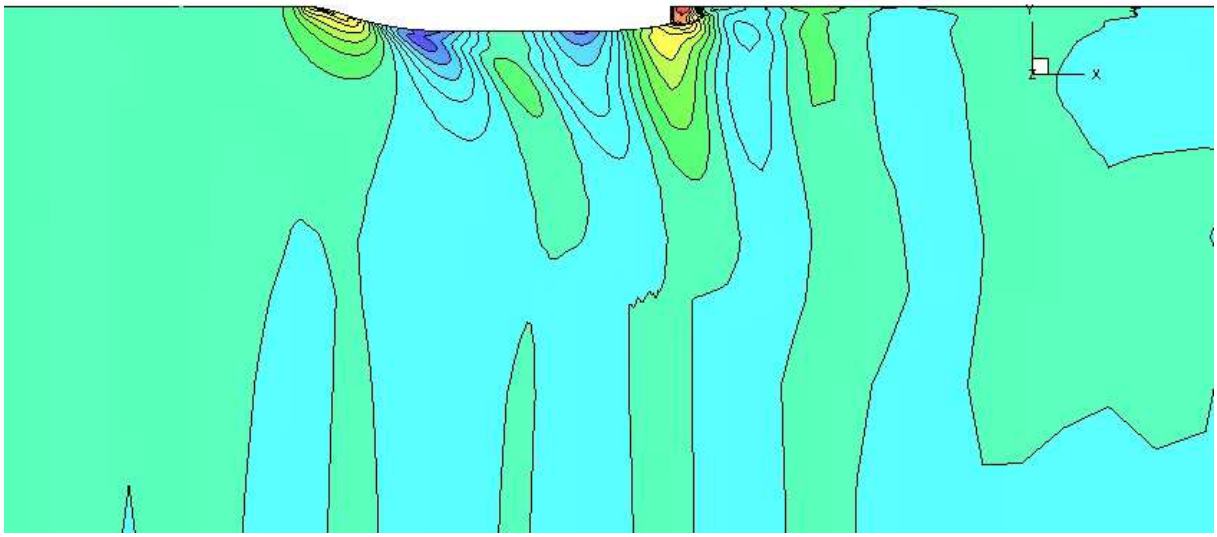

Figure 41. Free surface for viscous flow at design speed 24 Knts.

Figure 42. Pressure distribution on the KCS body for viscous flow at design speed 24 Knts.

The calculations of total ship viscous resistance coefficients has been attained by the SHIPFLOW, and the total resistance is calculated using the formulae:

$$R_T = \frac{1}{2}\rho * S * C_T * V^2 \qquad \text{Eq. 46}$$

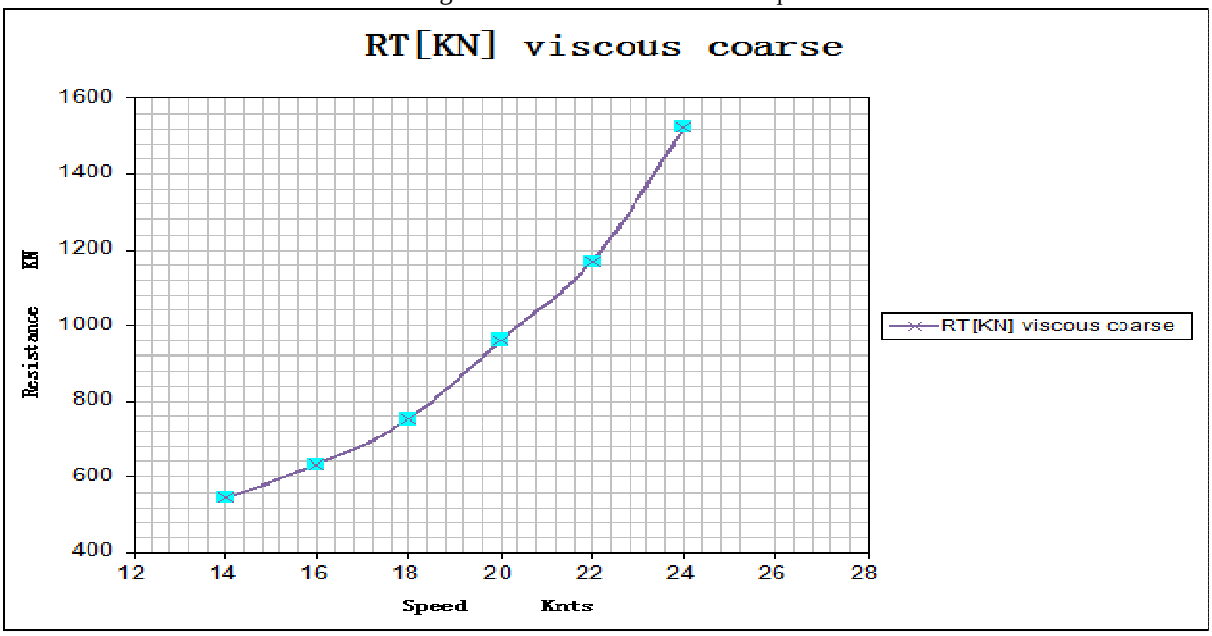

Figure 43. Ship resistance for viscous flow.

5 Resistance test with KCS model

Ship resistance tests are done all over the world on ship models and the accuracy of the results is a complex problem which includes a number of factors. One of these factors is the choice of the modelling scale that imposes directly the dimensions of the ship model.
The Towing Tank at the Faculty of Naval Architecture of the Dunarea de Jos University of Galati has small size; the main dimensions are 45 x 4 x 3 m, with an automated towing carriage which has restriction of towing ship models not more than 200 kg and 4 m in length.

5.1 Experimental methodology

The ship resistance tests carried in calm water are influenced by experimental errors for physical modelling. These errors are: *systematic errors* as the simplification of assumptions made for the experimental conditions, the errors from instruments, etc., and *random nature errors* as the environmental factors like temperatures, pressure and humidity.
The selection of the model scale is a very sensitive issue in the experimental modelling, it is held in conjunction with a need to achieve several requirements, like reducing the scale impact and the modelling of few parameters which influence the ship resistance, and also the experimental equipment locations etc.
The errors of measurements can increase by decreasing the length of the model which influences the Froude similitude and Reynolds similitude by the effects coming from the scale.
The towing tank of the Naval Architecture Faculty, from *Dunarea de Jos* University of Galati, has a small size of (45 x 4 x 3). It has a modern carriage manufactured by Cussons Technology from UK, with a maximum speed up to 4m/s. This carriage has an automatic driving system and a computer program for data acquisition and analysis.
In the Figures 44-45 represent the towing tank of the University of Galati and the KCS model during the test.

Figure 44. Towing tank at the University of Galati.

Figure 45. The KCS model during the resistance test.

The KCS model in the University of Galati was built for scale of 1/65.67, the length between perpendiculars of this model is 3.502 m, based on ITTC 7.5-01-01-01 recommendations. The model is not equipped by any appendages or devices as propeller, rudder or turbulence producers. Also, the ship model was free related to heave and pitch motions. The blockage factor was not considered.

The KCS ship hull was proposed firstly as a benchmark ship by the ITTC and has been studied by the Korean research institute KRISO now MOERI based on their experimental model which has length of 7.279 m (1/31.5995 model scale) [3].

Between the results of the two towing tanks experiments we have done a comparative analysis, in order to evaluate the accuracy of prediction of a small towing tank as the one of the University of Galati.

The resistance test was carried in the Galati's towing tank at a temperature of 18°C. The Figure 46-47 are for the ship KCS model.

The ITTC 1957 method has been used in order to transpose the resistance results obtained in the KRISO towing tank, for the 7.279 m experimental model, at the Galati's 3.502 m experimental model scale.

Figure 46. KCS model forward part.

Figure 47. KCS model aft part.

5.2 Model tests results

The following Table 40 presents the results from the experimental resistance test performed at the UGAL towing tank, at a temperature of 18°C, where R_{m0} is "zero" value of the resistance

dynamometer, $R_{m\ stab}$ is the constant value of the stabilized signal and R_m is the total resistance of the model, obtained as the difference between R_{m0} and $R_{m\ stab}$.

Table 40. Experimental results for KCS model resistance test.

Vs [Knts]	Vm [m/s]	R_{m0} [N]	$R_{m\ stab}$ [N]	R_m [N]
16	1.02	2.555	-2.726	5.281
18	1.14	2.425	-3.723	6.148
20	1.27	2.490	-5.055	7.545
22	1.40	2.662	-6.517	9.179
24	1.52	2.797	-8.430	11.227
26	1.65	2.886	-12.426	15.312

The following Figure 48 represents the resistance results from the model test, depending of the ship speed.

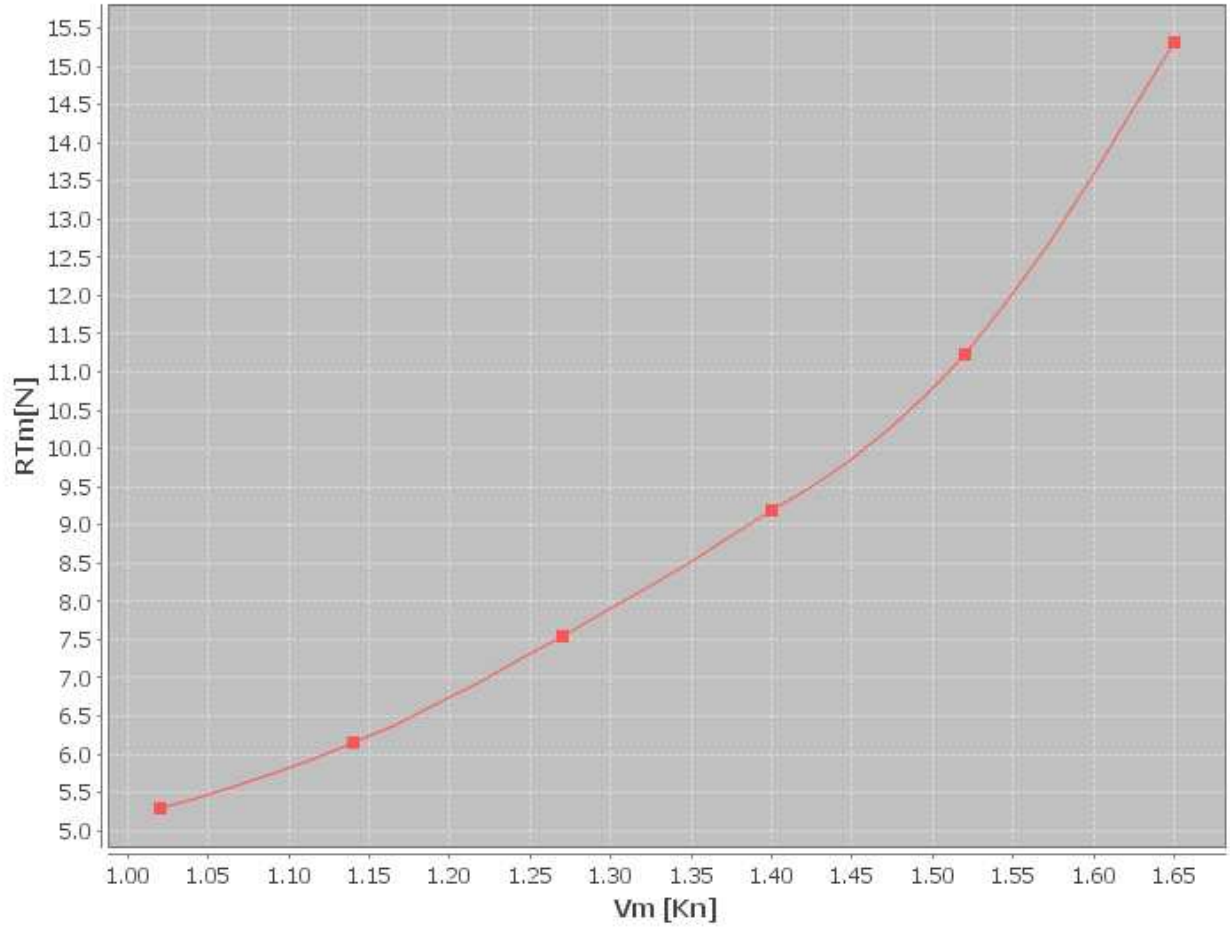

Figure 48. Resistance of the model test in UGAL.

The experimental results obtained in the towing tank of Galati with the model of 3.502 m in length were compared with KRISO results for the model of 7.279 m in length (see Table 41and Figure 49). The KRISO results were transposed at the scale of Galati model, using ITTC 1957 method. The differences D [%] are presented in the last column and decrease if the model speed is increased.

Table 411. Comparative results for KCS model resistance test.

Vs [Knts]	$R_{mGALATI}$ [N]	R_{mKRISO} [N]	D [%]
16	5.281	4.666	13.2
18	6.148	5.699	7.9
20	7.545	7.026	7.4
22	9.179	8.680	5.7
24	11.227	10.581	6.1
26	15.312	14.635	4.6

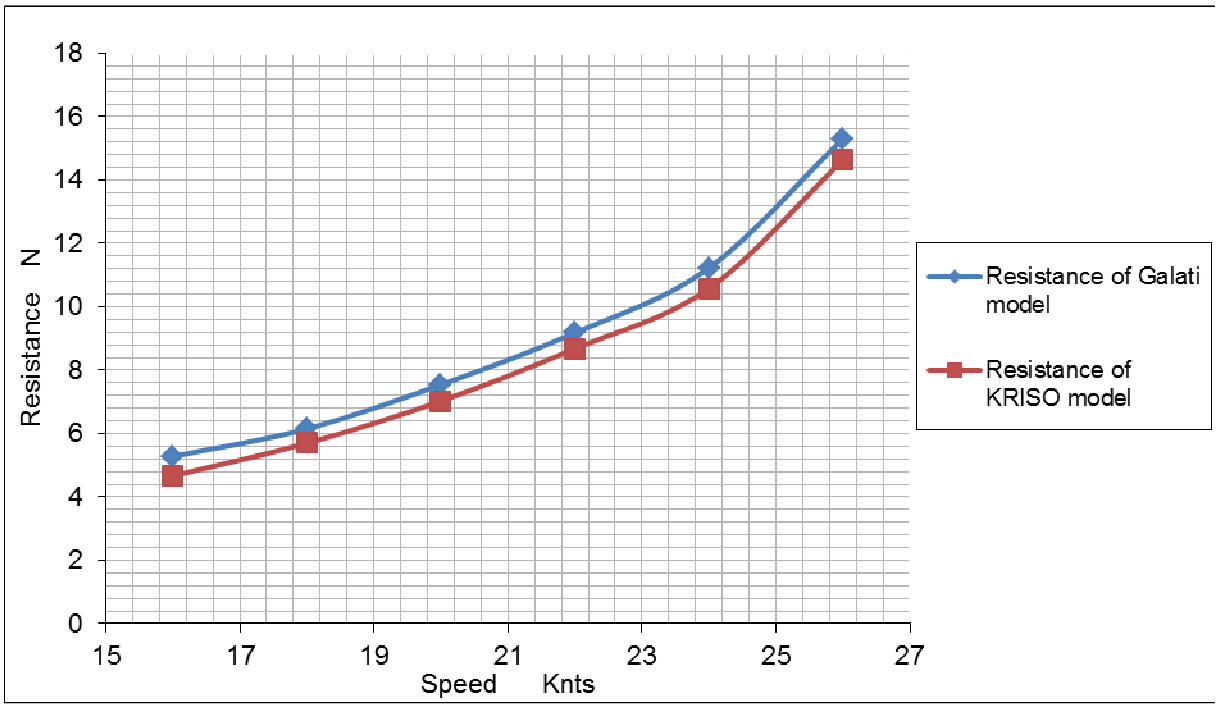

Figure 49. Comparative results for KCS model resistance test.

5.3 Numerical and experimental comparative results

The comparison of the full scale results obtained from the UGAL towing tank tests for a 3.502 m model and from the KRISO institute for a 7.279 m model is analysed, based on the ITTC 1957 method. The results are transposed to the full scale at 15°C.

The results transposed from resistance test in the towing tank of University of Galati are plotted in the Figure 50.

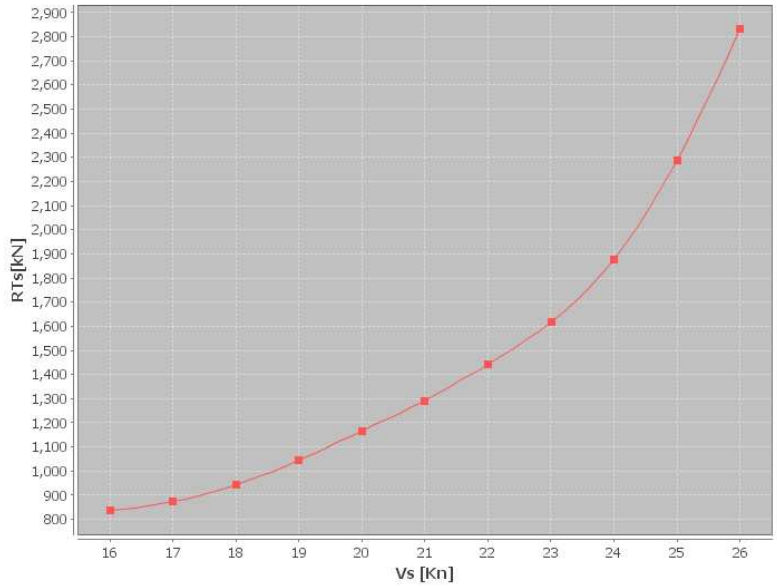

Figure 50. KCS Resistance transposed to full scale from Galati towing test.

Also, the effective power is obtained and shown in the Figure 51.

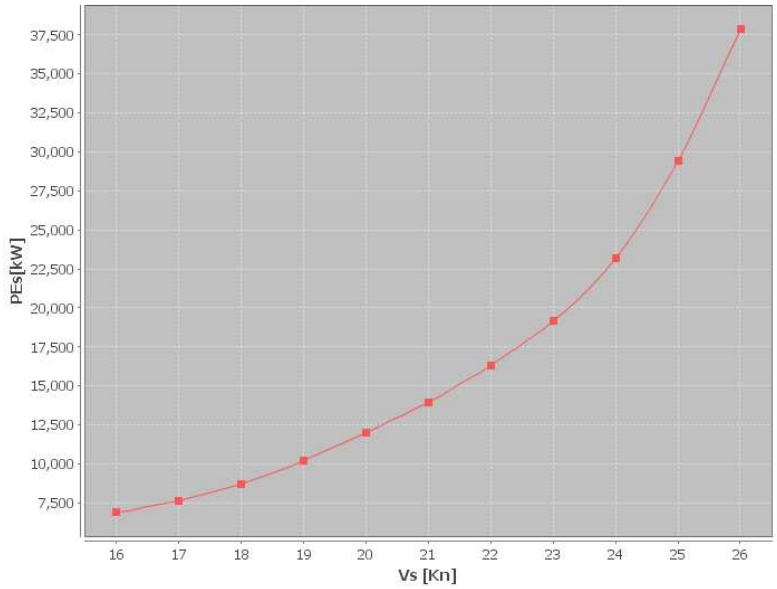

Figure 51. Effective power transposed to full scale.

The different calculations of the KCS full scale resistance (in KN) from Galati towing tank test, Tribon-M3, Viscous flow, are compared in the following Tables 42-43, where the difference is noted as D in percentage.

Table 42. Comparative results Galati Tribon-M3.

	Galati	Tribon	D %
Vs [Knts]	RTs [KN]	RTs[KN]	
16	836,934	715,8671	16,9
17	874,03	818,9519	6,7
18	938,772	935,6769	0,3
19	1044,316	1067,661	-2,2
20	1167,994	1217,556	-4,1
21	1292,218	1386,134	-6,8
22	1451,701	1572,457	-7,7
23	1617,191	1784,129	-9,4
24	1857,949	2035,469	-8,7
25	2289,283	2332,714	-1,9
26	2827,303	2661,636	6,2

Table 43. Comparative results Galati Viscous flow.

	Galati	viscous	D %
Vs	RTs		
16	836,934	633,2488769	32,2
17	874,03	676,7705926	29,1
18	938,772	752,7271087	24,7
19	1044,316	848,8425254	23,0
20	1167,994	961,4719738	21,5
21	1292,218	1052,398939	22,8
22	1451,701	1169,134072	24,2
23	1617,191	1313,430584	23,1
24	1857,949	1523,355895	22,0
25	2289,283	1733,281205	32,1
26	2827,303	1943,206516	45,5

These comparative results are shown in the graph in the following Figure 52.

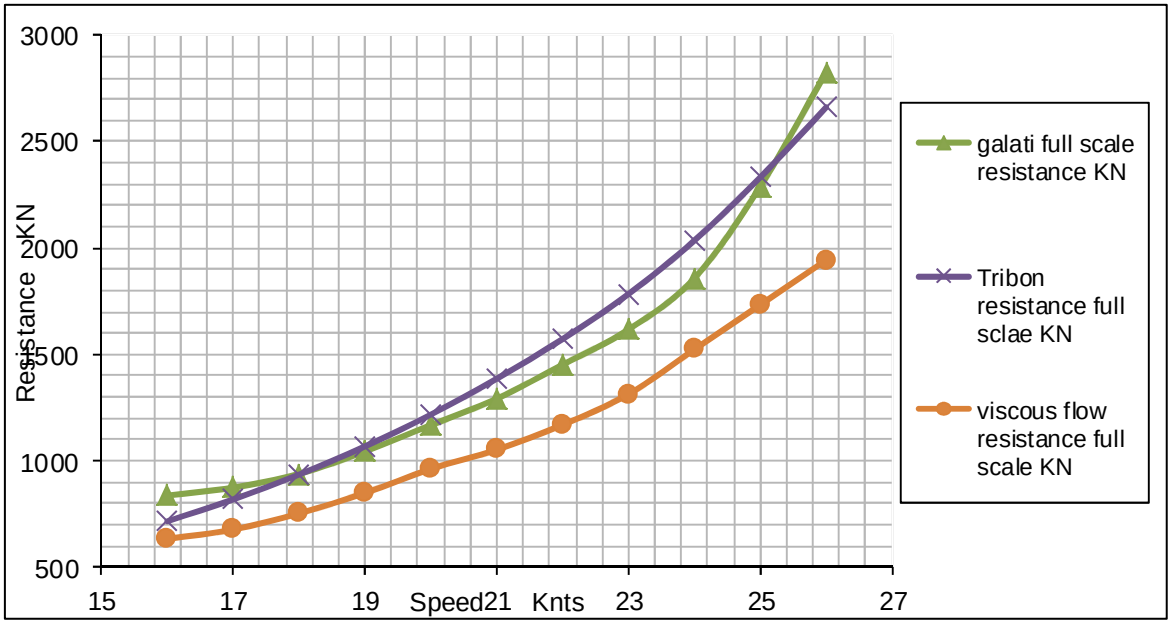

Figure 52. Comparative Graphs of resistance.

From these comparative results we observe:

_ The Galati towing tank ship resistance test curve has an ascending slope.

_ From all the above comparison we find that the nearest results to the Galati Towing tank results are the Tribon-M3 resistance results.

6 Conclusion

The prediction and validation of the hydrodynamic performances of KRISO KCS container ship was the objective of this thesis and it was carried using different tools: CAD-CAE (TRIBON-M3) and CFD techniques.

From this study we may conclude:

- The calculations of the total resistance have been carried by using the AVEVA Tribon-M3 system at the design speed, using the Holtrop and Mennen method. Thus for the optimum propeller calculations in open water condition the Wageningen B-Series method was used.
- Referring to the IMO criteria and in the Tribon-M3, the analysis of the manoeuvring performances (ZIG-ZAG manoeuvre, Turning circle test, spiral manoeuvre) we found that the KCS container ship has good manoeuvring properties.
- Using the CFD SHIPFLOW code, the analysis of the potential flow free surface around the KCS hull has been performed, for different sets of grids and for a range of speed between [14 Knts – 26 Knts].
- Using the CFD SHIPFLOW code, the analysis of the viscous flow free surface around the KCS hull has been performed, for one set of grid and for a range of speed between [14 Knts – 24 Knts].
- The most important issue for the resistance tests is the accuracy of results, and the important factor which has influence is the modelling scale by imposing the ship model dimensions. The towing tank of the Faculty of Naval Architecture at the University of Galati allows tests for models not exceeding 4 m length. So in this the chances of having accurate results should be evaluated. In this thesis the comparative results and analysis between the resistance test at Galati University and KRISO and also with numerical methods is done to increase the confidence in our results. We conclude that this analysis can be done in small towing tanks as the UGAL, with satisfactory accuracy from educational view point.

As a final conclusion we can conclude that the numerical predictive tools of initial design or CFD both are recommended for use in naval architecture domain, because it covers a very large domain of studies and it has proved its proficiency and accuracy.

For future recommendations: we can suggest the seakeeping calculations, the calculation of the hydrodynamic derivatives, also the CFD calculations for different sets of grids in Viscous flow analysis.

7 REFERENCES

Journal article	[1]. Tomasz Bugalski, Pawel Hoffmann, "**Numerical Simulation Of The Self-Propulsion Model Tests**", Ship Design and Research Centre S.A. (CTO), Gdansk, Poland.
	[5] LARSSON, L., RAVEN, H., C. (2010): **The Principles of Naval Architecture Series: Ship Resistance and Flow**. The Society of Naval Architects and Marine Engineers, USA
	[6] Pechenyuk, A.W., "**Computation Of Perspective KRISO Container Ship Towing Tests With Help Of The Complex Of The Hydrodynamical Analysis Flow Vision**", Digital Marine Technology.
Book	[7] Volker Bertram, 2000 **Practical Ship Hydrodynamics** , Butterworth-Heinemann Linacre House, Jordan Hill, Oxford OX2 8DP 225 Wildwood Avenue, Woburn, MA 01801-2041 A division of Reed Educational and Professional Publishing Ltd
	[8] Edward V.Lewis Editor, 1989, **principles of naval architecture**, Volume III motion in waves and controllability.
Chapter	[9] MENTER, F.R. (1993): **Zone Two Equation k-w Turbulence Models for Aerodynamic Flows**, 24th Fluid Dynamics Conference, Orlando, AIAA paper-93- 2906.
	[10] VERSTEG, H. K., MALALASEKERA, W. (1995): **An Introduction to Computational Fluid Dynamics**, Longman Scientific & Technical, Essex, England.
	[11] Florin PACURARU, Adrian LUNGU, Ana-Maria Tocu, phd Student, 2008, **, approach for the numerical modelling of the flow around a liner ship hull** 4th Workshop on Vortex Dominated Flows Bucharest, Romania September 12 - 13, 2008 HYBRID BEM-RANKINE SOURCE
Internet document	[12] Michael S. Triantafyllou Franz S. Hover, Latest Revision: January 11, 2002, **MANEUVERING AND CONTROL OF MARINE VEHICLES**, Department of Ocean Engineering Massachusetts Institute of Technology Cambridge, Massachusetts USA
Newspaper article	[3]. Dan Obreja, Oana Marcu, "**Resistance Tests In A Small Towing Tank With Kcs Model**", Dunarea de Jos University of Galati, Domneasca Street, N° 47, 800008, Romania.
	[4]. Vladimi I. Krasilnikov "Self-Propulsion RANS Computations With A Single-Screw Container Ship", 1Norwegian Marine Technology Research Institute (MARINTEK), Trondheim, Norway.
	[13] Zhi-rong Zhang, 2010 , "**Verification And Validation For RANS Simulation Of KCS Container Ship Without/With Propeller**", China Ship Scientific Research Centre, Wuxi, China, 9th international conference on hydrodynamics, October 11-15, 2010 shanghai, china.

Thesis	[2]. Hyunyul Kim, "Multi-Objective Optimization For Ship Hull Form Design", A dissertation submitted in partial fulfilment of the requirements for the degree of Doctor of Philosophy at George Mason University, Summer Semester 2009 George Mason University Fairfax, VA.
	[14] MICHAŁ ORYCH, Development of a Free Surface Capability in a RANS Solver with Coupled Equations and Overset Grids, THESIS FOR THE DEGREE OF LICENTIATE OF ENGINEERING Department of Shipping and Marine Technology CHALMERS UNIVERSITY OF TECHNOLOGY Göteborg, Sweden 2013
	[15] Mohammed Ramzi Chahbi , 2014, Hydrodynamics Forces and Moments on KVLCC2 Hull, with Drift Angle and Rudder Angle Influences, Master Thesis, developed at "Dunarea de Jos" University of Galati In the framework of the "EMSHIP"

APPENDICES

APPENDIX AN1 Table of hydrostatic calculations

Draft (m)	Displt (t)	LCB (m)	VCB (m)	WPA (m^2)	LCF (m)	KML (m)	KMT (m)	WSA (m^2)	TPC (t/cm)	MTC (t-m/cm)
0.50	1421.06	111.401	0.264	3149.85	112.294	3823.167	94.290	3217.07	32.29	236.20
1.00	3148.83	112.121	0.533	3559.26	113.029	2175.423	54.677	3699.39	36.48	297.76
1.50	5048.38	112.547	0.804	3840.20	113.447	1551.820	40.378	4072.77	39.36	340.44
2.00	7074.50	112.854	1.076	4059.37	113.775	1218.575	32.839	4399.61	41.61	374.49
2.50	9202.89	113.101	1.348	4241.52	114.056	1010.509	28.147	4700.98	43.48	403.79
3.00	11416.63	113.307	1.620	4392.88	114.262	865.515	24.884	4984.06	45.03	428.82
3.50	13702.16	113.480	1.892	4522.00	114.418	759.063	22.474	5255.65	46.35	451.08
4.00	16048.91	113.624	2.164	4633.24	114.504	677.347	20.621	5520.66	47.49	471.13
4.50	18449.88	113.737	2.435	4734.04	114.493	612.800	19.207	5782.82	48.52	489.62
5.00	20900.45	113.819	2.707	4828.00	114.383	561.249	18.106	6044.26	49.49	507.56
5.50	23398.28	113.868	2.978	4919.06	114.153	519.560	17.253	6306.70	50.42	525.53
6.00	25942.00	113.879	3.250	5007.50	113.781	484.901	16.594	6571.14	51.33	543.26
6.50	28530.70	113.848	3.523	5094.92	113.276	456.265	16.074	6839.22	52.22	561.61
7.00	31164.69	113.772	3.795	5184.83	112.573	432.880	15.679	7112.95	53.14	581.40
7.50	33846.52	113.643	4.069	5280.49	111.682	414.477	15.385	7394.70	54.13	603.95
8.00	36578.22	113.457	4.344	5380.66	110.581	399.917	15.165	7685.81	55.15	629.10
8.50	39364.53	113.208	4.621	5493.29	109.278	389.846	15.033	7989.77	56.31	659.31
9.00	42210.64	112.894	4.899	5615.51	107.783	383.324	14.958	8306.41	57.56	694.50
9.50	45122.43	112.511	5.180	5750.62	106.126	380.632	14.932	8637.12	58.94	736.58
10.00	48107.71	112.064	5.464	5899.00	104.506	382.339	14.935	8972.63	60.46	788.29
10.50	51170.76	111.565	5.750	6052.53	102.944	385.969	14.956	9310.49	62.04	845.92
10.80	53045.53	111.247	5.923	6136.06	102.189	386.721	14.974	9506.86	62.89	878.24
11.00	54308.74	111.032	6.039	6182.78	101.828	385.671	14.984	9630.90	63.37	896.41
11.50	57503.59	110.506	6.329	6276.95	101.348	379.406	15.008	9922.10	64.34	932.75
12.00	60739.91	110.015	6.617	6347.97	101.274	370.409	15.012	10196.20	65.07	960.73

APPENDIX AN2 Table of sectional area calculation of KCS

Trim 0.00 metres AP is at Station 0
Heel 0.00 degrees FP is at Station 10

Sectional Areas - sq.metres

WL Heights	0.00	1.00	2.00	3.00	4.00	5.00	6.00	7.00	8.00	9.00	10.00	10.80	11.00

Station													
0.000	0.000	0.000	0.000	0.000	0.000	0.000	0.000	0.000	0.000	0.000	0.000	1.515	3.660
0.250	0.000	0.000	0.000	0.000	0.000	0.000	0.466	1.833	2.775	3.271	6.049	17.529	21.735
0.500	0.000	0.637	3.058	5.873	8.409	10.324	11.615	12.546	13.681	16.648	28.469	46.538	51.819
0.750	0.000	1.631	5.393	9.665	13.971	18.118	22.094	26.201	32.035	43.141	63.520	85.251	91.087
1.000	0.000	3.382	8.551	14.324	20.357	26.612	33.388	41.465	52.487	70.224	95.945	119.776	125.948
1.500	0.000	6.161	14.819	24.945	36.353	49.304	64.342	82.513	105.269	132.987	163.810	189.331	195.758
2.000	0.000	9.581	22.807	38.457	56.425	76.951	100.493	127.317	156.954	188.293	220.365	246.125	252.565
2.500	0.000	13.774	32.235	53.967	78.395	105.259	134.249	164.896	196.567	228.673	260.857	286.616	293.056
3.000	0.000	18.915	42.760	69.582	98.546	128.984	160.415	192.398	224.578	256.778	288.978	314.738	321.178
3.500	0.000	24.037	51.984	81.828	112.862	144.631	176.750	208.944	241.144	273.344	305.544	331.304	337.744
4.000	0.000	27.197	57.360	88.786	120.814	153.006	185.206	217.406	249.606	281.806	314.006	339.766	346.206
5.000	0.000	28.370	59.246	91.100	123.281	155.481	187.681	219.881	252.081	284.281	316.481	342.241	348.681
6.000	0.000	23.691	51.241	80.650	111.247	142.608	174.457	206.577	238.777	270.977	303.177	328.937	335.377
6.500	0.000	19.957	44.180	70.670	98.783	128.127	158.396	189.346	220.800	252.603	284.643	310.360	316.796
7.000	0.000	15.664	36.163	59.167	84.068	110.466	138.083	166.724	196.237	226.459	257.272	282.270	288.560
7.500	0.000	11.420	27.671	46.356	66.892	88.997	112.474	137.205	163.057	189.933	217.757	240.660	246.474
8.000	0.000	7.427	19.202	33.304	49.080	66.212	84.531	103.976	124.538	146.236	169.092	188.214	193.109
8.500	0.000	4.292	11.933	21.444	32.240	44.032	56.672	70.112	84.375	99.559	115.778	129.576	133.148
9.000	0.000	2.321	6.548	12.086	18.638	25.892	33.603	41.599	49.799	58.275	67.281	75.086	77.142
9.250	0.000	1.570	4.820	9.254	14.642	20.737	27.242	33.890	40.398	46.658	52.862	58.070	59.442
9.500	0.000	1.033	3.405	6.799	11.062	16.000	21.323	26.575	31.274	35.223	38.753	41.601	42.340
9.750	0.000	0.576	2.646	5.789	9.821	14.492	19.511	24.472	28.893	32.253	34.429	35.832	36.202
10.000	0.000	0.236	1.976	4.863	8.661	13.067	17.785	22.462	26.584	29.178	29.277	29.265	29.264

WL Heights Station	12.00	13.00	14.00	15.00	16.00	17.00	18.00	19.00
0.000	23.341	50.312	80.283	111.725	143.791	175.994	182.113	182.113
0.250	47.256	76.651	107.712	139.535	171.670	203.870	209.988	209.988
0.500	80.557	111.480	143.362	175.541	207.741	239.941	246.059	246.059

WL Heights Station	12.00	13.00	14.00	15.00	16.00	17.00	18.00	19.00
0.750	121.507	153.099	185.147	217.336	249.536	281.736	287.854	287.854
1.000	157.487	189.590	221.789	253.989	286.189	318.389	324.507	324.507
1.500	227.958	260.158	292.358	324.558	356.758	388.958	395.076	395.076
2.000	284.765	316.965	349.165	381.365	413.565	445.765	451.883	451.883
2.500	325.256	357.456	389.656	421.856	454.056	486.256	492.374	492.374
3.000	353.378	385.578	417.778	449.978	482.178	514.378	520.496	520.496
3.500	369.944	402.144	434.344	466.544	498.744	530.944	537.062	537.062
4.000	378.406	410.606	442.806	475.006	507.206	539.406	545.524	545.524
5.000	380.881	413.081	445.281	477.481	509.681	541.881	547.999	547.999
6.000	367.577	399.777	431.977	464.177	496.377	528.577	534.695	534.695
6.500	348.989	381.189	413.389	445.589	477.789	509.989	516.107	516.107
7.000	320.211	352.125	384.255	416.455	448.655	480.855	486.973	486.973
7.500	276.028	306.293	337.174	368.595	400.388	432.439	438.874	438.874
8.000	218.277	244.581	272.001	300.481	329.935	360.305	391.409	422.834
8.500	151.800	171.868	193.495	216.807	241.879	268.709	296.727	325.396
9.000	88.132	100.496	114.478	130.317	148.256	168.485	190.542	213.625
9.250	66.814	75.332	85.294	97.003	110.670	126.318	143.922	162.777
9.500	46.358	51.214	57.276	64.866	74.282	85.762	99.114	113.839
9.750	38.200	40.645	43.680	47.646	52.743	59.324	67.506	77.328
10.000	29.349	29.591	30.075	31.008	32.681	35.316	39.075	44.042

Vertical Moments of Sectional Areas - cub. metres

WL Heights Station	0.00	1.00	2.00	3.00	4.00	5.00	6.00	7.00	8.00	9.00	10.00	10.80	11.00
0.000	0.000	0.000	0.000	0.000	0.000	0.000	0.000	0.000	0.000	0.000	0.000	16.187	39.582
0.250	0.000	0.000	0.000	0.000	0.000	0.000	2.695	11.578	18.586	22.801	49.795	169.833	215.689
0.500	0.000	0.503	4.207	11.247	20.080	28.639	35.694	41.734	50.298	75.827	189.238	377.556	435.119
0.750	0.000	1.135	6.855	17.553	32.619	51.266	73.132	99.863	143.893	238.923	433.331	659.540	723.154
1.000	0.000	1.963	9.793	24.256	45.387	73.563	110.895	163.555	246.586	398.068	642.970	890.917	958.190
1.500	0.000	3.398	16.530	41.952	81.992	140.417	223.336	341.767	512.866	748.834	1041.808	1307.248	1377.306
2.000	0.000	5.244	25.303	64.619	127.707	220.303	350.053	524.681	747.141	1013.620	1318.332	1586.236	1656.432
2.500	0.000	7.449	35.446	90.019	175.729	296.811	456.414	655.733	893.326	1166.238	1471.989	1739.885	1810.081
3.000	0.000	10.052	46.123	113.385	214.907	351.980	524.912	732.829	974.188	1247.888	1553.788	1821.692	1891.888
3.500	0.000	12.544	54.672	129.396	238.085	381.094	557.762	767.023	1008.523	1282.223	1588.123	1856.027	1926.223
4.000	0.00	14.0	59.4	138.0	250.1	395.0	572.1	781.4	1022.9	1296.6	1602.5	1870.4	1940.6

WL Heights Station	0.00	1.00	2.00	3.00	4.00	5.00	6.00	7.00	8.00	9.00	10.00	10.80	11.00
	0	25	13	51	76	43	43	43	43	43	43	47	43
5.000	0.000	14.552	60.982	140.670	253.311	398.211	575.311	784.611	1026.111	1299.811	1605.711	1873.615	1943.811
6.000	0.000	12.424	53.944	127.586	234.754	375.931	551.132	759.927	1001.426	1275.126	1581.026	1848.930	1919.126
6.500	0.000	10.575	47.140	113.519	212.032	344.167	510.713	711.934	947.877	1218.225	1522.623	1790.085	1860.230
7.000	0.000	8.533	39.533	97.219	184.515	303.416	455.402	641.647	863.061	1119.993	1412.764	1672.764	1741.330
7.500	0.000	6.383	31.007	77.891	149.909	249.503	378.734	539.581	733.560	962.088	1226.493	1464.728	1528.103
8.000	0.000	4.298	22.197	57.612	112.952	190.148	290.998	417.487	571.795	756.324	973.549	1172.463	1225.829
8.500	0.000	2.571	14.225	38.129	76.006	129.145	198.732	286.159	393.204	522.349	676.524	820.076	859.006
9.000	0.000	1.404	7.863	21.806	44.810	77.499	119.939	171.932	233.451	305.528	391.139	472.359	494.771
9.250	0.000	0.990	5.970	17.151	36.078	63.551	99.354	142.562	191.347	244.550	303.504	357.689	372.650
9.500	0.000	0.663	4.312	12.878	27.860	50.129	79.423	113.529	148.716	182.226	215.746	245.371	253.432
9.750	0.000	0.430	3.634	11.574	25.752	46.812	74.444	106.655	139.742	168.197	188.757	203.354	207.384
10.000	0.000	0.200	2.922	10.223	23.582	43.446	69.408	99.788	130.628	152.480	153.370	153.244	153.233

WL Heights Station	12.00	13.00	14.00	15.00	16.00	17.00	18.00	19.00
0.000	266.871	604.361	1009.148	1465.125	1962.186	2493.538	2598.127	2598.127
0.250	509.673	877.305	1296.725	1758.203	2256.297	2787.610	2892.197	2892.197
0.500	765.866	1152.532	1582.980	2049.580	2548.680	3079.980	3184.567	3184.567
0.750	1073.122	1468.092	1900.753	2367.499	2866.599	3397.899	3502.486	3502.486
1.000	1320.970	1722.279	2156.970	2623.870	3122.970	3654.270	3758.857	3758.857
1.500	1747.603	2150.112	2584.812	3051.712	3550.812	4082.112	4186.699	4186.699
2.000	2026.732	2429.232	2863.932	3330.832	3829.932	4361.232	4465.819	4465.819
2.500	2180.381	2582.881	3017.581	3484.481	3983.581	4514.881	4619.468	4619.468
3.000	2262.188	2664.688	3099.388	3566.288	4065.388	4596.688	4701.276	4701.276
3.500	2296.523	2699.023	3133.723	3600.623	4099.723	4631.023	4735.610	4735.610
4.000	2310.943	2713.443	3148.143	3615.043	4114.143	4645.443	4750.030	4750.030
5.000	2314.111	2716.611	3151.311	3618.211	4117.311	4648.611	4753.199	4753.199
6.000	2289.426	2691.926	3126.626	3593.526	4092.626	4623.926	4728.513	4728.513
6.500	2230.459	2632.959	3067.659	3534.559	4033.659	4564.959	4669.546	4669.546
7.000	2105.331	2504.287	2938.053	3404.944	3904.044	4435.344	4539.931	4539.931
7.500	1868.028	2246.404	2663.340	3118.992	3611.802	4140.654	4250.706	4250.706
8.000	1515.347	1844.241	2214.503	2627.558	3084.163	3585.341	4129.708	4711.090
8.500	1073.617	1324.591	1616.689	1954.862	2343.630	2786.450	3276.840	3807.253
9.000	621.254	775.930	964.832	1194.661	1472.901	1806.876	2192.967	2620.078
9.250	457.507	564.090	698.705	868.647	1080.660	1339.011	1647.233	1996.143

WL Heights Station	12.00	13.00	14.00	15.00	16.00	17.00	18.00	19.00
9.500	299.687	360.480	442.430	552.626	698.725	888.326	1122.118	1394.632
9.750	230.393	261.000	302.040	359.624	438.737	547.460	690.806	872.624
10.000	154.223	157.267	163.825	177.415	203.404	246.973	312.851	404.850